2. Evolution of a major segmented normal fault during multiphase rifting: The origin of plan-view zigzag geometry

Gijs A. HENSTRA [1,*], Atle ROTEVATN [1], Robert L. GAWTHORPE [1], Rodmar RAVNÅS [2]

[1] *Department of Earth Science, University of Bergen, Allégaten 41, 5007 Bergen, Norway*

[2] *A/S Norske Shell, Tankvegen 1, 4056 Tananger, Norway*

Abstract

This case study addresses fault reactivation and linkage between distinct extensional episodes with variable stretching direction. Using 2-D and 3-D seismic reflection data we demonstrate how the Vesterdjupet Fault Zone, one of the basin-bounding normal fault zones of the Lofoten margin (north Norway), evolved over c. 150 Myr as part of the North Atlantic rift. This fault zone is composed of NNE-SSW- and NE-SW-striking segments that exhibit a zigzag geometry. The structure formed during Late Jurassic and Early Cretaceous rifting from selective reactivation and linkage of Triassic faults. A rotation of the overall stress field has previously been invoked to have taken place between the Triassic and Jurassic rift episodes along the Lofoten margin. A comparison to recent physical analogue models of non-coaxial extension reveals that this suggested change in least principal stress for the Lofoten margin may best explain the zigzag-style linkage of the Triassic faults, although alternative models cannot be ruled out. This study underlines the prediction from physical models that the location and orientation of early phase normal faults can play a pivotal role in the evolution of subsequent faults systems in multi-rift systems.

1. Introduction

The evolution of normal faults (initiation, propagation, linkage) is traditionally described as the progressive incidental coalescence of growing fault segments that started off as geometrically and kinematically independent structures. This process has been documented for both outcrop and seismic studies (e.g. Peacock and Sanderson, 1991; Cartwright et al., 1996; McLeod et al., 2000; Young et al., 2001) as well as modeling studies (e.g. Scholz et al., 1993; Crider and Pollard, 1998; Cowie et al., 2000). Linkage through propagation of initially unrelated faults has recently been referred to as the 'isolated fault model' (Walsh et al., 2003). The alternative 'coherent fault model' describes how a soft-linked fault array can form as a system that is kinematically linked since initiation (Morley et al., 1999; Walsh et al., 2002, 2003). The coherent fault model can explain how a pre-existing, large fault at depth can be reactivated in such a way that, at surface, new faults develop that are soft-linked (e.g. Giba et al., 2012; Jackson and Rotevatn, 2013).

Propagation and linkage of faults involves the destruction of relay ramps. Such overlap zones between normal faults are formed and obliterated throughout the formation of a normal fault zone (Peacock and Sanderson, 1991; Childs et al., 1995); this is a continuous process that occurs without a change in the overall extension vector, and regardless of whether the fault system forms via the isolated or the coherent fault model. Physical models simulating uniform extension typically yield mostly parallel structures with minor lateral steps (Keep and McClay, 1997; Henza et al., 2011). The parallel geometries of faults growing under uniform extension was observed in nature by Acocella et al. (2000), who stated that in their study area, the combined length of parallel normal faults would have to be less than fourteen times their strike-normal separation in order for the faults to interact.

In contrast, physical models simulating the effects of various degrees of non-coaxial extension revealed that, after a change in the direction of extension, widely spaced first phase faults would link up to produce fault systems with strong zigzag or cross-

cutting plan-view geometries (Henza et al., 2011). While the pivotal role of (oblique) reactivation has now been investigated extensively in physical models (see also Dubois et al., 2002), natural examples from the geological record are rare. This mode of linking fault segments may explain some types of zigzag fault patterns as commonly seen in rift systems (e.g. Freund and Merzer, 1976; Lepvrier et al., 2002; Jackson et al., 2002; Morley et al., 2004, 2007; Bergh et al., 2007; Whipp et al., 2014).

This study investigates the c. 100 km long Mesozoic Vesterdjupet Fault Zone (VFZ; Blystad et al., 1995) which forms the main border fault to the North Træna Basin. The spatio-temporal relationship between its constituent segments is presently not well known. Bergh et al. (2007) argue that differently striking fault populations of the Lofoten margin reflect distinct rift pulses (see also: Eig and Bergh, 2011 and Færseth, 2012). More specifically, they suggest that the NNE-SSW-striking segments of the VFZ predate NE-SW-striking segments, with the latter forming transfer faults linking the former. In contrast, Wilson et al. (2006) suggest that the differently striking segments of Mesozoic normal faults of the Lofoten margin could have formed simultaneously as conjugate sets under a uniform stress field, locally perturbed by an inherited Caledonian basement grain or a transfer zone.

We have mapped the hanging wall to the VFZ in detail using an extensive database of old, reprocessed as well as recently acquired 2-D and 3-D seismic reflection surveys. The VFZ and its constituent parts have been reactivated repeatedly; the tectonic style of the Triassic and Jurassic rift episodes has therefore been overprinted by Cretaceous rifting. Specific structures within its hanging wall, on the other hand, record only these earlier rift episodes, after which activity on them ceased. We assume that these abandoned hanging wall faults and the precursors to the VFZ evolved similarly prior to Cretaceous rifting. The abandoned hanging wall faults are therefore used as proxies for the evolution of the proto-VFZ during the Triassic and Jurassic rift episodes.

Our results show that each subsequent Mesozoic rift episode is associated with reactivation of structures from the foregoing episode, as well as inception of new faults. We thus support the model of Bergh et al. (2007), and demonstrate how the VFZ, with its characteristic zigzag plan-view geometry, formed by reactivation and linkage of Triassic faults during subsequent rift events in the Late Jurassic and Early Cretaceous. By comparing the results of this case study to recent physical models simulating coaxial- and non-coaxial extension, we aim to carry insights from such analogues to the understanding of natural rifts. We present several scenarios for the origin of zigzag geometries of segmented normal faults and discuss alternative models for fault growth and the influence of a change in extension direction.

2. Geological Setting

2.1 The Lofoten segment of the Norwegian passive continental margin

The Norwegian passive continental margin forms part of the eastern side of the greater North Atlantic, which evolved during Palaeozoic-Mesozoic continental rifting and eventual breakup in early Cenozoic times. This complex tectonic history resulted from divergent plate motions between Eurasia and Laurentia during breakup of Pangea (Doré, 1992), which in the North Atlantic was largely accomplished by a rift along the Caledonian suture (Doré, 1992; Torsvik and Cocks 2003).

The Lofoten-Vesterålen margin segment is bordered to the southwest and northeast by the continental continuations of oceanic transform zones (Mosar et al., 2002). To the southwest, the Bivrost Lineament separates it from the greater Vøring Basin and the Trøndelag platform, whereas to the northeast the margin segment is bordered by the Senja Fracture Zone, which forms part of the western Barents Sea transform margin (Doré et al., 1997; Olesen et al., 2002). This study focuses on the shelfal area west of the Lofoten Islands (Fig. 1; herein referred to as the Lofoten margin).

The contractional phase of the Caledonian Orogeny was replaced by a phase of orogenic collapse and exhumation of thickened crust in Devonian times (Andersen et al., 1991; Fossen, 2000), which lasted until the Permian in the Lofoten area (Hames and Andresen, 1996), at which time it was facilitated by the development of a metamorphic core complex (Hames and Andresen, 1996; Steltenpohl et al., 2004; Henstra and Rotevatn, 2014). Subsequently the area between Greenland and Norway experienced recurring episodes of rifting that alternated with periods of relative tectonic quiescence or uplift (Lundin and Doré 1997; Brekke, 2000; Faleide et al., 2008).

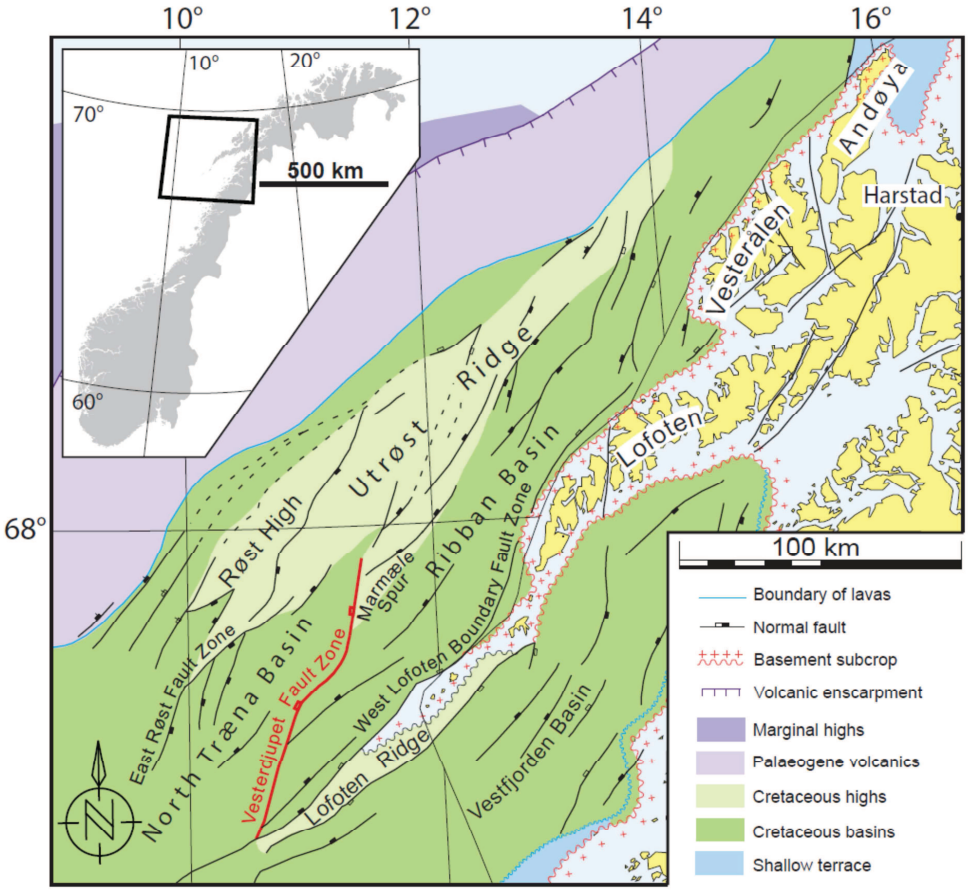

Fig. 1. *Structural element map of the Lofoten-Vesterålen segment of the Norwegian passive continental margin. Modified after Blystad et al. (1995).*

The late Permian to earliest Cretaceous interval of the Lofoten margin is subdivided into two main rift episodes (Hansen et al., 1992; Hansen et al., 2012; Færseth, 2012), very similar to the Northern North Sea and Mid Norwegian margin: i) a latest Permian to Early Triassic episode and ii) a Middle Jurassic to earliest Cretaceous episode. In the Lofoten Margin, another rift event occurred towards the end of the Early Cretaceous (Hansen et al., 1992; Blystad et al., 1995; Løseth, H., Tveten, 1996; Doré et al., 1999; Tsikalas et al., 2001).

The initial framework of Hansen et al. (1992), in which two distinct periods of rifting are recognized in the Early Cretaceous, has been adopted by several more recent studies (Koch and Heum 1995; Brekke 2000, Tsikalas et al., 2001, Surlyk, 2003). However, two alternative schools of thought exist; following Doré (1992), Lundin and Doré (1997), Doré et al. (1999) and Hansen et al. (2012), the Early Cretaceous is characterised by a period of rifting that began in the Valanginian. Rifting cessation is associated with a middle Cenomanian erosional event. Færseth (2012) on the other hand argues that the Lower Cretaceous itself resembles post-rift basin-fill, with fine-grained marine sediments infilling sediment-starved, inactive half-grabens inherited after Late Jurassic rifting. Our results indicate that the nature of the lower part of the Lower Cretaceous fits the model of Færseth (2012), but that the upper part of the Lower Cretaceous records an important rift episode during which Triassic and Jurassic faults were reactivated and linked up to form large, segmented fault zones.

A final rift episode occurred in Campanian to Palaeogene across the Norwegian continental shelf (Skogseid et al., 2000; Færseth and Lien, 2002; Gernigon et al., 2003). In the Lofoten margin widespread fault block rotation resulted in reinvigorated activity along the major basin bounding fault systems that govern the half-graben architecture of the Lofoten margin (Tsikalas et al., 2001; Færseth, 2012; Hansen et al., 2012).

2.2 Evolution of the regional stress regime during the Mesozoic

The Permo-Triassic rift episode of the northern North Atlantic is characterised by E-W directed extension (Mosar et al., 2002; Coward et al., 2003; Faleide et al., 2010). For the Lofoten margin specifically, NNE-trending structures of this age have been documented both onshore (Steltenpohl et al., 2004; Wilson at al., 2006) and offshore (Hansen et al., 1992; Færseth, 2012; Hansen et al., 2012).

For the Lofoten margin a change in extension direction has been invoked for the Late Jurassic to Early Cretaceous rift episode based on the development of NE-SW- to E-W-striking faults in addition to continued activity of NNE-SSW-striking ones (Tsikalas et al., 2001; Bergh et al., 2007), similar to other areas of the Norwegian continental shelf (Færseth et al., 1997; Clifton et al., 2000). This suggests that since the Permo-Triassic rift episode, the extensional stress field vector had rotated c. 30-50° clockwise. This stress rotation was also invoked by Faleide et al. (2008), who emphasise its regional, NE Atlantic-Arctic nature. Alternatively, Færseth (2012) and Hansen et al. (2012) interpret inception of NE-SW- to E-W-striking faults in the Lofoten margin during the Late Jurassic to Early Cretaceous to represent linkage of NNE-SSW-striking segments and see no evidence for an overall regional stress rotation.

A change in the direction of absolute plate motions occurred c. 85 Ma (Torsvik et al., 2001b). This has been suggested to have caused (another) change in the regional stress regime, towards NW-SE to NNW-SSE directed extension, during the Campanian-Palaeocene rift episode and continental break-up in the Eocene (Mosar et al., 2002). The timing and orientation of this change in extension direction is agreed upon by different workers; it resulted in activity of NE- to ENE-trending faults in the Lofoten margin (Tsikalas et al., 2005; Wilson et al., 2006; Bergh et al., 2007; Færseth, 2012).

2.3 The North Træna Basin and the Vesterdjupet Fault Zone

The North Træna Basin is a prominent half-graben (Fig. 2), bounded by the VFZ and the Marmæle Spur to the east and the East Røst Fault Zone (ERFZ; *sensu* Hansen et al., 2012; Fig. 1) to the northwest, which separates the basin from the Røst High. The ERFZ is smaller, both in length (17 km) and offset (500 m), than the VFZ which measures a total length of 100 km, and a maximum offset of almost 3500 m. South of the Marmæle Spur, the VFZ juxtaposes the North Træna Basin against the southern Ribban Basin. The southern extension of the VFZ is buried deeply underneath the Upper Cretaceous Træna Basin proper and is not well imaged where it meets the SW-

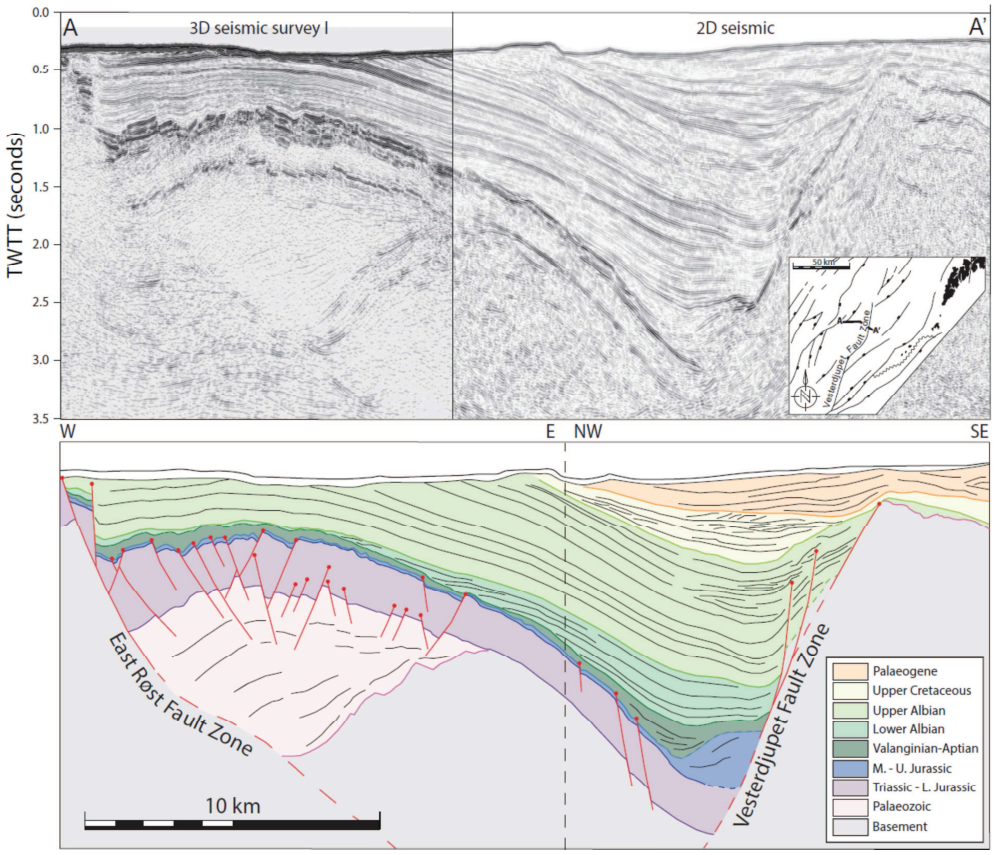

Fig. 2. *Composite geoseismic section (A-A') across the North Træna Basin; location is indicated in Figure 3. Stratigraphic subdivision largely follows that of Hansen et al. (1992). With the exception of the mid-Albian, all Mesozoic and Palaeogene events are tied to well data; see text for details.*

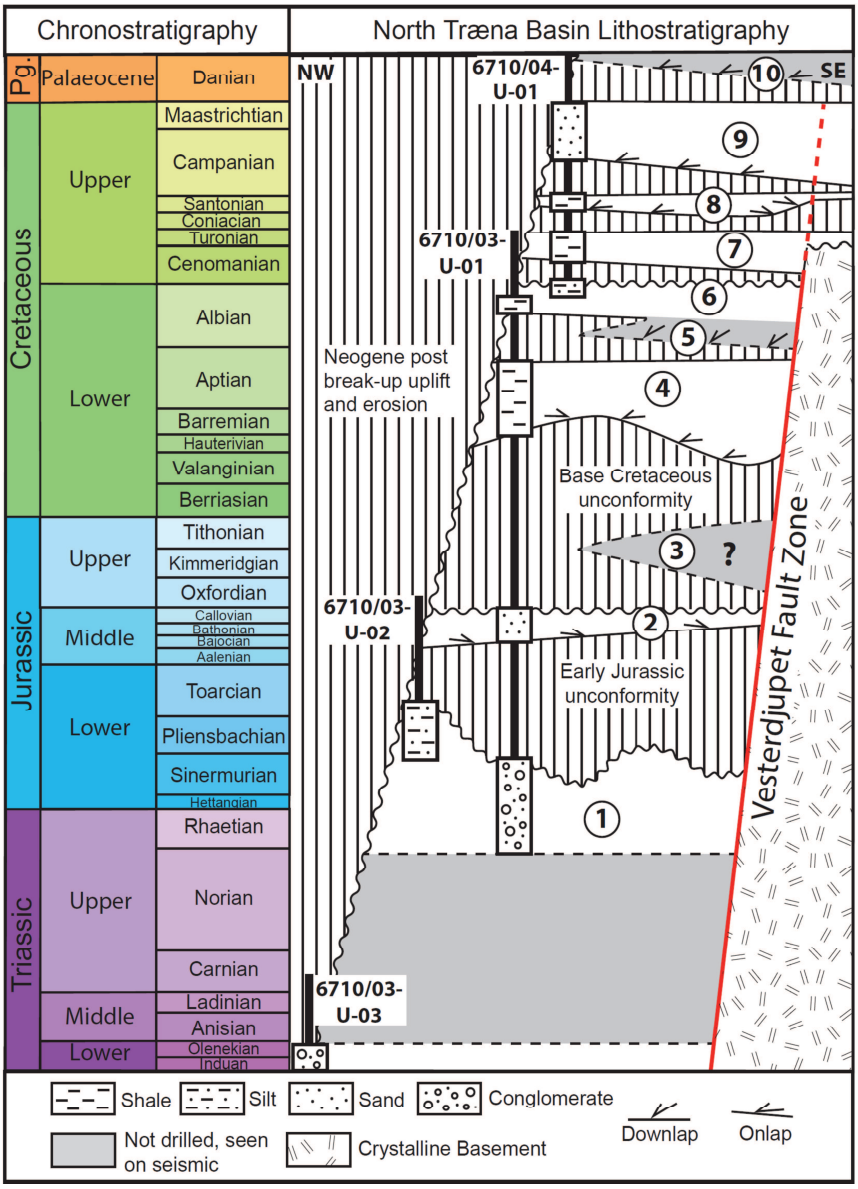

Fig. 3. *Chart of stratigraphic sequences and events of the North Træna Basin. This chart is based on the sequences encountered by the shallow cores (Hansen et al., 1992), combined with seismic stratigraphy. 1: Triassic-lower Jurassic (Åre Fm.); 2: middle Jurassic (Melke Fm.); 3: upper Jurassic (Spekk Fm.); 4: Valanginian-Aptian (Lyr/Lange Fm.); 5: lower Albian (Lange Fm.); 6: upper Albian (Lange Fm.); 7: Cenomanian-Turonian (Lange Fm.); 8: Santonian (Nise Fm.); 9: Campanian-Maastrichtian (Springar Fm.); 10: Palaeocene (Tang Fm.). See text for full discussion.*

trending Lofoten Ridge (Blystad et al., 1995; Færseth, 2012; Hansen et al., 2012). To the north the fault zone loses displacement into a series of splays over the Utrøst Ridge. Both the Marmæle Spur and the Røst High connect to the Utrøst Ridge, a Cretaceous high (Blystad et al., 1995) lying to the north of the North Træna Basin.

A lack of well data hampers our understanding of the tectonostratigraphy of the Lofoten-Vesterålen margin. Shallow boreholes were drilled by the Norwegian continental shelf institute (IKU) in the early 1990s to address this. The stratigraphic subdivision as established by IKU (Hansen et al., 1992) is used as a starting point of this study. Figure 3 provides an overview of the tectono-sequences and events based on boreholes and additional seismic observations.

Earliest Triassic sediments rest on crystalline basement in most of the area. This contact has a clear seismic expression and forms the lower boundary to an isopachous interval observed on seismic (Fig. 2). The upper portion of this interval consists of the uppermost Triassic and Lower Jurassic Åre Fm. A Middle Jurassic erosional surface has cut down to the Lower Jurassic (Fig. 3).

The Middle Jurassic is present across the basin; where drilled, the Middle Jurassic sequence is overlain by Cretaceous strata, meaning that the Upper Jurassic is absent. Away from the drilled area, however, the Jurassic sequence expands (Fig. 2) and an additional, presumably Upper Jurassic sequence is present between the Middle Jurassic and Base Cretaceous seismic horizons (Fig. 3). This sequence was penetrated further to the NE, in the northern Ribban Basin (Hansen et al., 1992).
Barremian age sediments overly the Base Cretaceous seismic horizon where drilled (Hansen et al., 1992). This contact is regionally known as the Cimmerian unconformity, which formed as a result of a widespread erosional or non-depositional event around early Valanginian times (Brekke, 2000). On seismic we observe that older strata onlap the Base Cretaceous away from the well location. These strata are conformable with the drilled Barremian sediments and are thus interpreted to be part of the same sequence, albeit older (Fig. 3). A correlation to the Lower Cretaceous

outcrops of Andøya has been proposed (Hansen et al., 2012), suggesting older portions of this onlapping sequence may be of Valanginian age. At the drilled location, the Barremian is overlain by shales of Aptian and Albian age (Hansen et al., 1992). On a seismic line that was acquired over the location of the well* the Barremian and Aptian shales are conformable. An unconformity is recognized on seismic to the SW of the well that, in the well, would separate the Aptian shales from the Upper Albian shales. Biostratigraphic data indicate that this lacuna spans the Early Albian (Hansen et al., 1992). The Upper Albian interval is isopachous and can be traced on seismic across the North Træna basin (Fig. 2). Away from the drilled location there are areas where an additional, wedge-shaped stratigraphic interval is observed between the Barremian-Aptian and Upper Albian successions of the well (Fig. 2). It is suggested that this wedge is of Early Albian age, and that it formed at the same time as the Aptian-Albian hiatus of the drilled location (Hansen et al., 1992). An (Upper) Albian age is also assigned to the lower portion of well 6711/04-U-01, based on the presence of a biostratigraphic assemblage that is similar to that of the Albian upper part of 6710/03-U-01.

The top of this Albian sequence is marked by a stratigraphic break, dated as middle Cenomanian (the Lower Cenomanian is absent or condensed). This break is associated with an unconformity that is observable on seismic data (Fig. 2; Hansen et al., 1992). The Upper Cretaceous consists of three sequences separated by two low-angle unconformities (Fig. 3).

3. Data & Methods

The seismic database used in the present study (Fig.4) includes pre-stack time-migrated 2-D and 3-D reflection seismic surveys. The line spacing of 2-D seismic data varies from 1 to 7 km; most surveys consist of lines oriented NW-SE, perpendicular to the coastline, with some NE-SW-oriented tie lines. The total length

** for a well to seismic tie the reader is referred to Figure 5 in **paper 3** (page 87)*

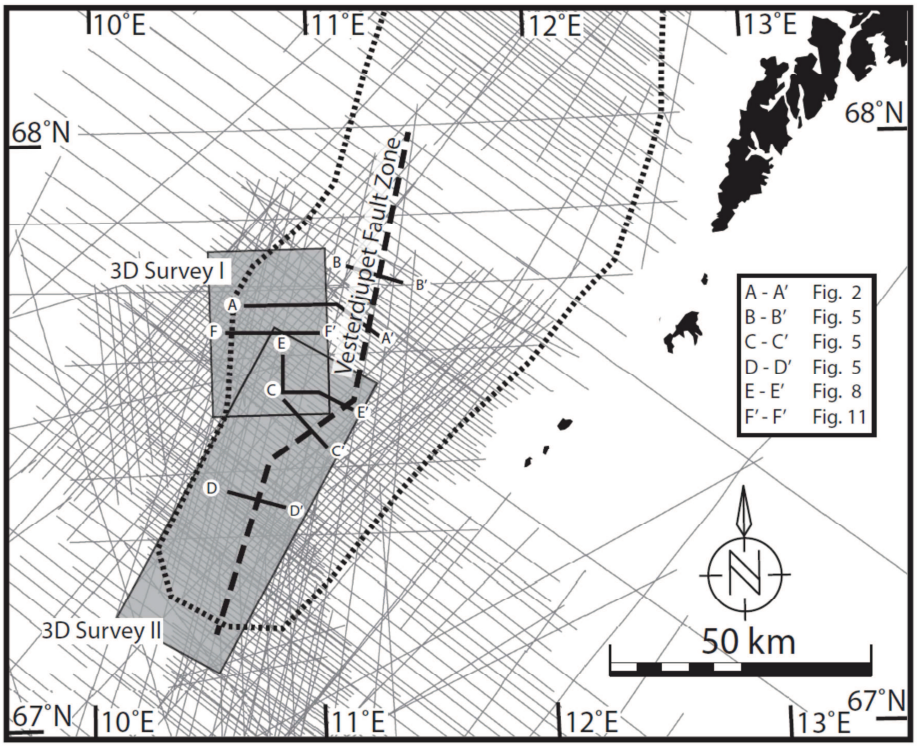

Fig. 4. *Base map showing the reflection seismic and well database used in this study; black lines and grey boxes refer to 2-D and 3-D reflection seismic data, respectively. Locations of cross sections shown in other figures are indicated in annotated solid black lines. Maximum extent of mapping (the area of interest) is indicated by the dotted black line. The stippled line indicates the location of the VFZ at Base Cretaceous level.*

of 2-D lines used is approximately 2000 km. Two 3-D reprocessed reflection seismic surveys that cover areas of c. 700 km^2 (NH9604; survey I) and 1500 km^2 (TBN99; survey II) are also used. The surveys have an inline and crossline spacing of 12.5 m; inlines are orientated E-W (survey I) and WNW-ESE (survey II), approximately perpendicular to fault strike, and cross-lines are orientated N-S and NNE-WSW respectively, approximately parallel to fault strike. The dominant frequency around the Base Cretaceous is c. 25 Hz. With an interval velocity of 3000 m/s the vertical resolution of the Upper Mesozoic is c. 60 m.

One of the objectives of this study is to resolve temporal activity along the VFZ in order to determine its spatiotemporal evolution. Normal fault activity controls

changes in the location and amount of accommodation (e.g. Ravnås et al., 2000). This is reflected in changes in the distribution and architecture of syn-tectonic strata, thus the sedimentary record of the hanging wall can be used to unravel the tectonic history of a segmented fault system (Prosser, 1993; Young et al., 2001). Seismic observations of stratigraphic thickening towards a structure directly indicate syn-tectonic sedimentation. Where applicable, expansion indices (Thorsen, 1963) have been calculated; these are used to quantify growth history of faults by comparing thickness of stratigraphic sequences between foot- and hanging wall (e.g. Groshong, 1999; Jackson and Rotevatn, 2013).

4. Tectonostratigraphy of the greater North Træna Basin

4.1 Structural framework

The Base Triassic horizon is recognized on seismic only in certain areas. The Base Cretaceous, on the other hand, forms a conspicuous seismic reflection throughout most of the North Træna Basin. It typically forms the contact between the Middle Jurassic and the Lower Cretaceous (Fig. 3), and thus often records cumulative strain of both the Late Jurassic and the Early Cretaceous rift episodes.

The overall WNW-dipping VFZ is comprised of a NE-SW-oriented central segment flanked by two NNE-SSW-oriented segment to the north and south (Fig. 5A). The three segments range from 15 to 60 km in length (Fig. 1), with throws averaging 2 km and with a throw maximum of 3.5 km (for the Base Cretaceous horizon) near the Marmæle Spur (Fig. 5B). The fault zone displays significant along-strike variability in structural style and distribution of total strain (Fig. 5A). Along the central segment, (Cretaceous) displacement is largely localized onto a single fault; elsewhere it is distributed across several faults that bound fault terraces of 10 – 15 km length and 0.4 to 3 km width (Fig. 5A). The NW edge of the basin is formed by the ESE-dipping ERFZ. This fault zone consists of a series of splays that come together in the NNE (Fig. 1), where its throw reaches a maximum of 750 m. Further to the NNE the ERFZ continues for 50 km across the Utrøst Ridge and forms the eastern border of the Røst

High (Hansen et al., 2012). Large portions of the fault zone and its foot- and hanging wall have been eroded following Palaeogene uplift.

4.2 Triassic – Lower Jurassic tectonostratigraphy of the North Træna Basin

The Base Triassic horizon and the Triassic-Jurassic isopach are strongly affected by younger tectonic and erosional events. As a consequence of the high level of uncertainty, fault polygons have not been created for this horizon. Thickness changes in the Triassic-Jurassic occur mostly gradual over tens of kilometres (Fig. 7A); some more abrupt changes can be linked to the presence of faults. Separating Early Triassic fault offset from more recent tectonic imprints has proven to be one of the main challenges of this study.

Triassic fault 1 of Figure 8 is characterized by strong differences in thickness of the Triassic – Lower Jurassic succession between foot- and hanging wall (Figs. 5C and 8). Moreover, the Triassic – Lower Jurassic interval exhibits thickening towards that fault. The Middle Jurassic, on the other hand, is an isopachous package of parallel reflections and exhibits no difference in thickness across the fault. The base of the Middle Jurassic resembles an angular unconformity at the footwall crest. The stratigraphic thickening of the Triassic – Lower Jurassic interval points at accommodation being generated by fault movement during deposition. Naturally, the hanging wall received most of the syn- and post-rift Triassic and Lower Jurassic

Fig. 5 *(following page). (A) TWTT map of the Base Cretaceous horizon. This horizon is gridded from interpretations performed on various 2-D and 3-D seismic reflection surveys; the interpretation grid (inset map) is shown as a measure of mapping resolution. (B) B-B' shows the NNE-SSW-striking northern segment that is characterized by a series of parallel terraces. (C) C-C' shows the NE-SW-striking central segment where the VFZ consists of one single fault plane. (D) D-D' shows the NNE-SSW-striking southern segment, where the VFZ is represented by two distinct fault planes.stratigraphic wells.*

(a)
TWTT (s)
1.0
2.0
3.0
4.0
11°E
12°E
13°E
68°00'N
67°30'N
25 km
Lofoten Islands
Utrøst Ridge
Ribban Basin
northern segment
6710/3-U-2
6710/3-U-3
6710/3-U-1
6711/4-U-1
East Røst Fault Zone
Fig. 10
Central Fault Zone
N. Træna Basin
southern segment
100 km
shallow borehole
100 ms contours
Base Cretaceous eroded in Neogene
Base Cretaceous fault polygons
B
WNW
B'
ESE
Vesterdjupet Fault Zone
TWTT (s)
0.0
0.5
1.0
5 km
(b)
C
NW
C'
SE
Triassic fault 1
(c)
D
WNW
D'
ESE
Palaeogene
U. Cretaceous
U/L. Albian
Valanginian-Aptian
U. Jurassic
M. Jurassic
Triassic/L. Jurassic
Syn-Rotational Strata
Jurassic ENE-WSW fault
(d)

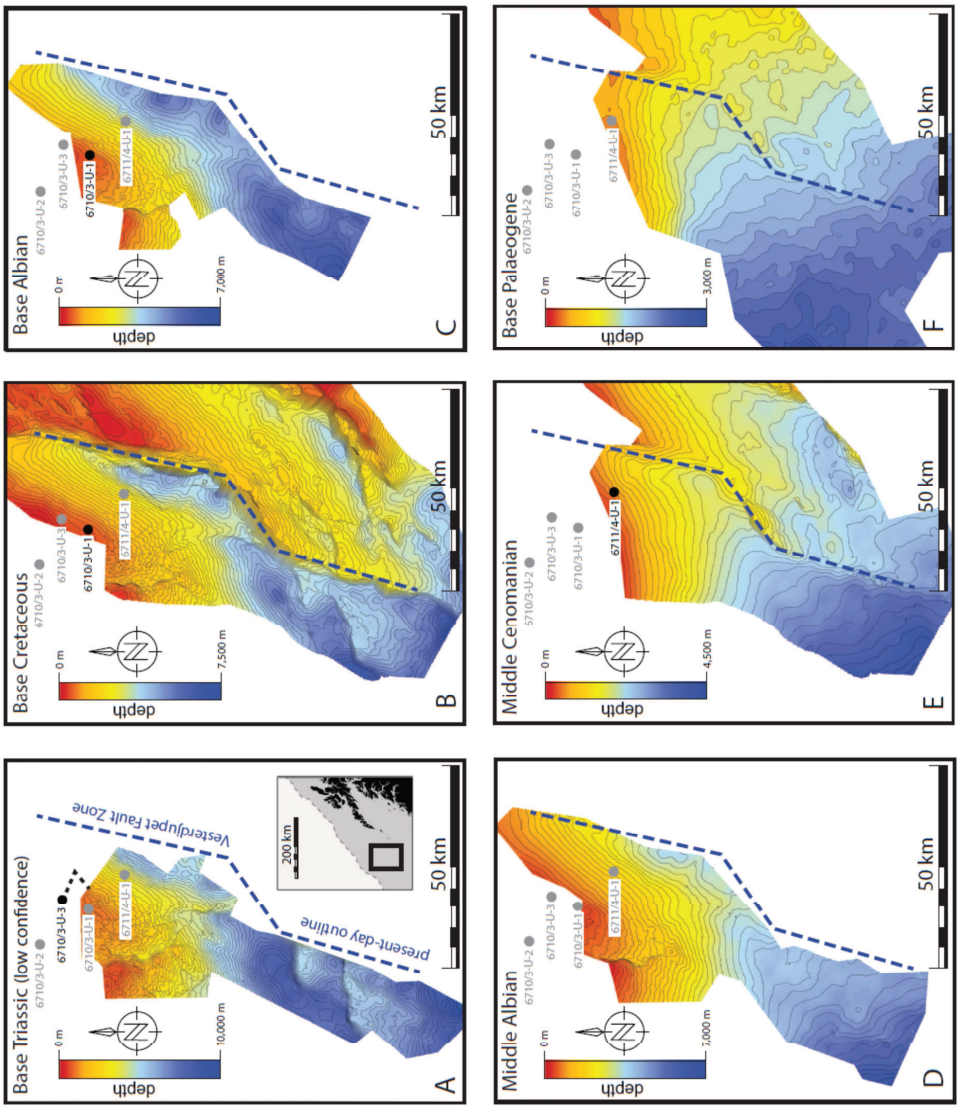

Fig. 6. *Depth converted structure maps for several Mesozoic events. The confidence of the Base Triassic horizon is low. Wells in black are used as starting point for that specific event. Contour spacing is 100 m. To the north, most of the horizons have been eroded in Palaeogene times. The SW border of these horizon maps is a picking limit; horizons plunge deep and seismic resolution is insufficient for reliable mapping. (A) The base Triassic horizon was drilled by 6710/3-U-3 and is tied to 3-D survey I by 2-D lines. The Base Triassic is only mapped in the hanging wall to the VFZ. (B) The Base Cretaceous was drilled by 6710/3-U-1 and is mapped also on the footwall of the VFZ and into the Ribban Basin. (C) The base Albian horizon was drilled by 6710/3-U-1 and is only mapped in the hanging wall to the VFZ. (D) The middle Albian has not been tagged by any well and is only mapped in the hanging wall to the VFZ. (E) The middle Cenomanian was drilled by 6710/3-U-1 and can be traced around the VFZ into the Ribban Basin. (F) The Base Palaeogene has been tagged by wells to the south of the study area (e.g. 6610/7-1; Eidvin et al., 1998).*

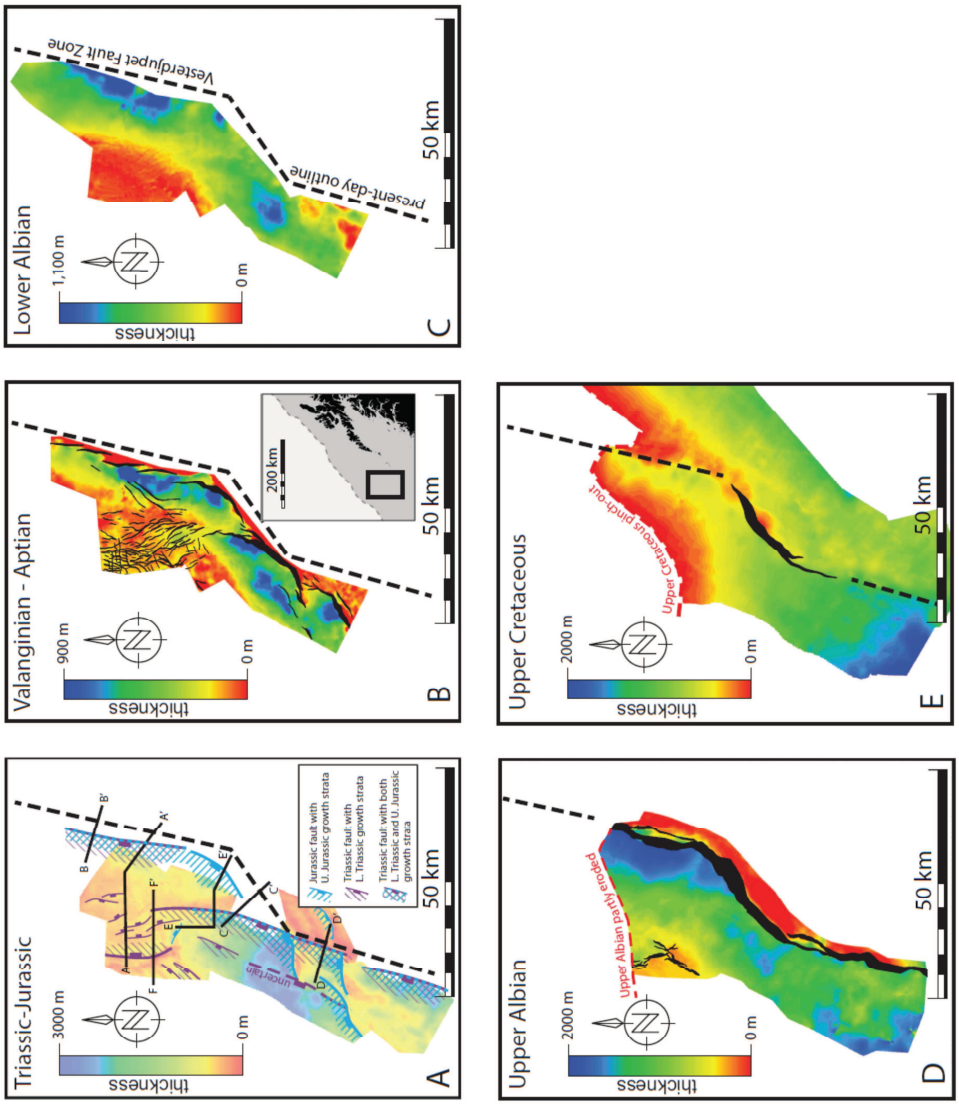

Fig. 7. *Isopach maps for the Mesozoic succession. The Base Triassic horizon is uncertain, for which reason the Triassic-Jurassic color scheme is faded. Fault offset of this isopach has not been mapped in detail, for which reason faults are indicated by lines rather than fault polygons. For the Cretaceous, each interval is shown together with corresponding fault planes as mapped in Figure 5. (A) Triassic-Jurassic: areas of syn-tectonic sedimentation are hatched, see text for detailed explanation. (B) Valanginian-Aptian: this interval is interpreted resemble passive infill of the underfilled Late Jurassic basins. (C) Lower Albian. (D) Upper Albian. (E) Upper Cretaceous.*

sediments; this contrast is reinforced by Middle Jurassic uplift erosion, which removed some of the Triassic - Lower Jurassic from the footwall. Subsequently, the transgressive Middle Jurassic sequence was deposited equally over the eroded surface. Offset of the Middle Jurassic must have occurred at a later stage. The areal extent of growth strata observed in the Lower Triassic and Upper Jurassic intervals (e.g. Figs. 5 and 8) is mapped and indicated on Figure 7A. The presence of fault-bounded depocentres in these intervals together explain most of the thickness changes of the Triassic-Jurassic isopach. Using growth strata as a proxy for syn-tectonic sedimentation, the location and orientation of Triassic faults can be resolved. The ERFZ, certain portions of the VFZ and several faults were active during the Early Triassic rift episode (Fig. 7A). These Triassic faults strike NNE-SSW, are up to c. 20 km long with a maximum displacement of 300 m.

The northern segment of the VFZ locally displays growth in the lower Triassic portion of the hanging wall (Figs. 2, 5B and 7A). This growth is not as pronounced as that seen in Figure 8; the fault that must have formed the depocentre here may have been small compared to other Triassic faults. Nevertheless, this indicates that a NNE-SSW-striking Triassic fault existed as precursor to the northern segment. Parts of the hanging wall of the southern segment are also characterized by growth of the Lower Triassic interval. Lower Triassic thickening as seen in Figure 5D suggests that Triassic fault 1 (Fig. 5C and 8) continues to the south. These growth strata indicate that at least part of the southern VFZ segment first developed in Triassic times. Unlike the northern and southern segments, the NE-SW-striking central segment of the VFZ displays no thickening of the Triassic – Lower Jurassic succession in its hanging wall (Figs. 5C and 8). This suggests that, at that time, a precursor to this segment had not yet formed.

There is a certain correlation between the occurrence of Triassic faults on the one hand and the presence of underlying Palaeozoic sediments on the other; where Palaeozoic sediments underlie the Mesozoic, faults of Triassic age (and younger) are abundant (Figs. 2 and 9A).

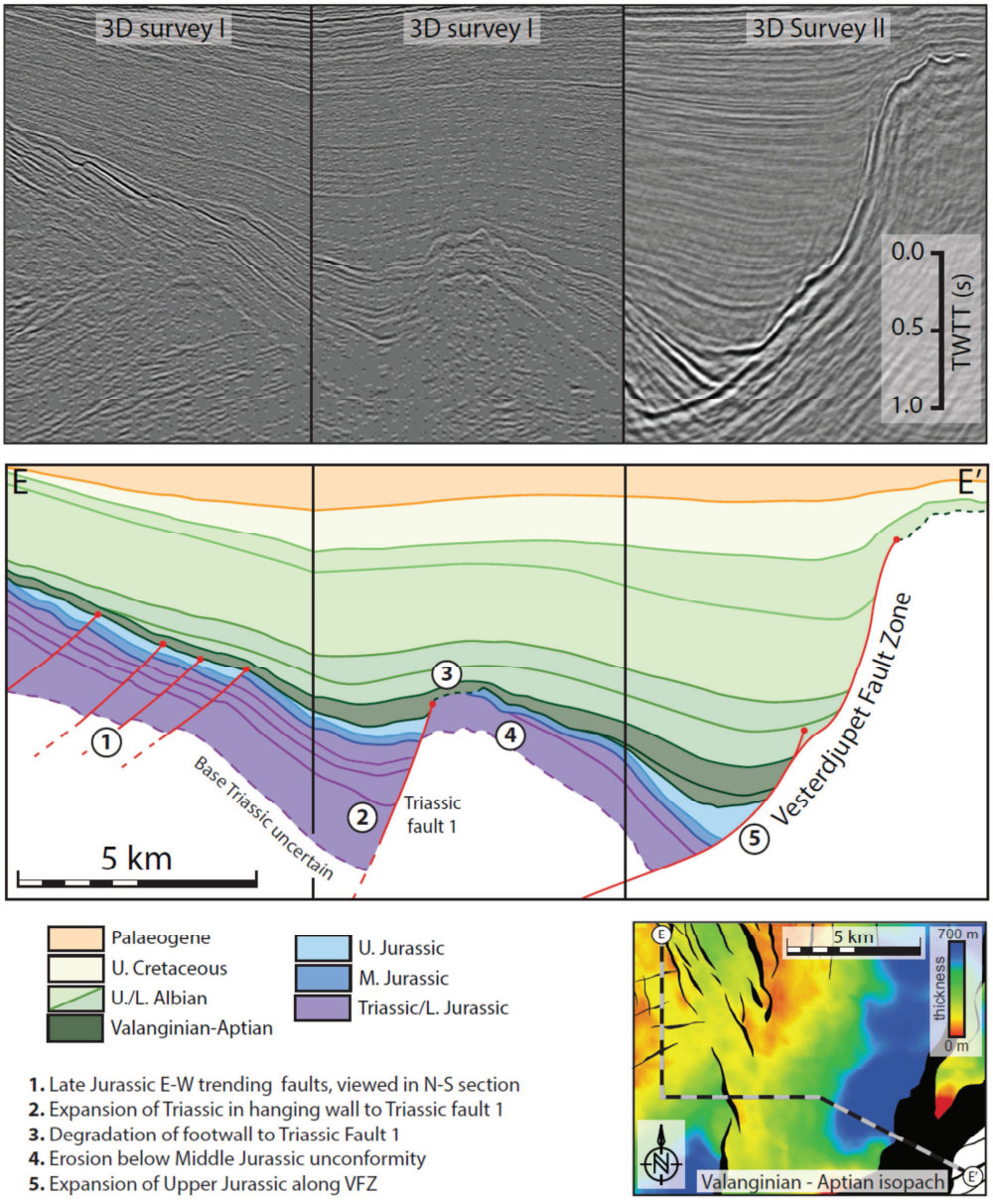

Fig. 8. *Geoseismic section E-E' across a series of faults in the North Træna Basin. Syn-tectonic 'growth' wedges indicate the faults were active in the Upper Jurassic. Note thickening of Triassic strata on the fault in the centre of the section (2), and unconformities that bear evidence of erosion of its footwall during Middle Jurassic (3) and Cretaceous (4) times. The VFZ to the right (5) shows syn-rotational deposition for both the Upper Jurassic and uppermost Albian intervals. Map location is indicated in Figure 10A. Note sharp angles between different portions of the cross-section, necessary to display faults at more or less perpendicular angles.*

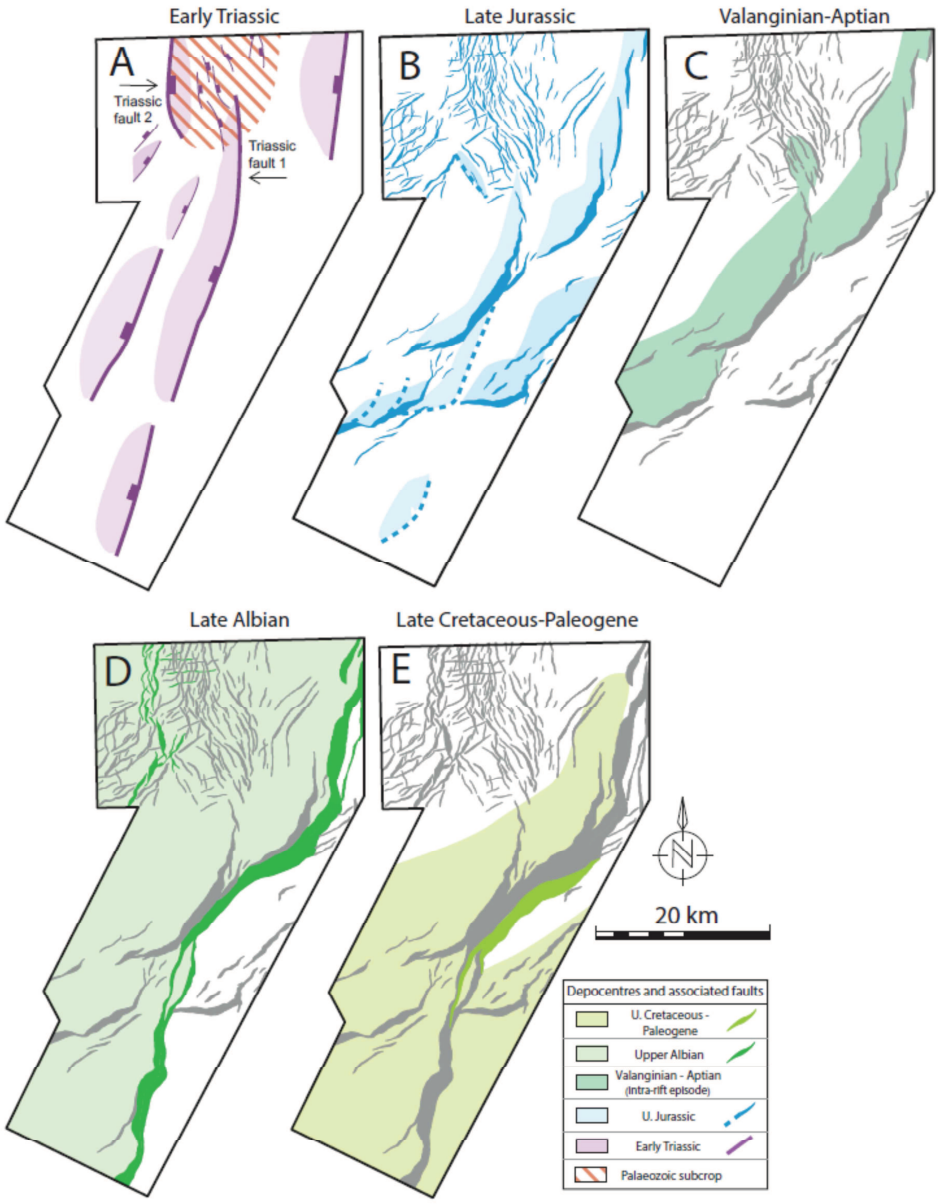

Fig. 9. *Summary figure showing the structural framework of the North Træna Basin as it evolved across the various rift episodes. (A) Triassic fault framework, taken from Figure 7A. (B) Late Jurassic fault framework. Fault polygons reflect those faults that are onlapped by Cretaceous sediments (Fig. 7B); lines reflect faults juxtaposed by Upper Jurassic strata (Fig 7A). (C) Depocentres of the Valanginian-Aptian intra/rift period. (D) Faults that were active during the Late Albian; the Late Jurassic fault polygons are included in grey. (E) Activity of the central segment of the VFZ as it occurred in late Cretaceous times; fault polygons of foregoing rift episodes are included in grey. See text for full discussion.*

4.3 Middle Jurassic – lowermost Cretaceous tectono-stratigraphy of the North Træna Basin

The Middle Jurassic is an isopachous interval with parallel reflections throughout the study area and is offset by numerous faults (Fig. 2). The Upper Jurassic, where present, is typically composed of growth strata (e.g. Fig. 8). These Upper Jurassic wedges are c. 10-15 km long, 5 km wide with a maximum thickness of 750 m. The overlying Valanginian-Aptian is characterised by abrupt thickness variations (from 0 to 450 m; Fig. 7B), but strata do not show thickening into faults that offset the Middle Jurassic. Instead, reflections are parallel and onlap/drape partly eroded Jurassic strata and exposed fault planes (Figs. 2, 5C, D and 8).

As described in the geological setting, different views exist on the timing of rifting at the Jurassic-Cretaceous transition. Given the syn-rift nature of the Upper Jurassic and the intra-rift nature of the Middle Jurassic and Valanginian-Aptian, we agree with Færseth (2012) that the lower part of the Lower Cretaceous resembles passive infill

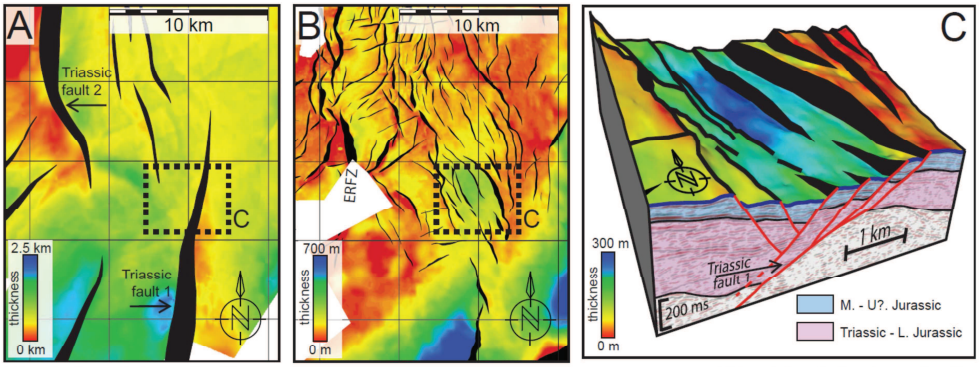

Fig. 10. *Late Jurassic reactivation of a Triassic fault. (A) Triassic-Jurassic isopach with fault polygons. 5 km grid is included for comparison between A and B. (B) Valanginian-Aptian isopach and associated fault polygons record Late Jurassic rift episode; note the right-stepping, en echelon array that has developed over Triassic Fault 1. See text for details. (C) Three-dimensional representation of the reactivated fault; the Valanginian-Aptian isopach map is projected onto the Base Cretaceous time structure map.*

of extensional basins formed during the Late Jurassic (see also Prosser, 1993). Faults that formed during the Late Jurassic rift episode are therefore identified from mapping fault-bounded Upper Jurassic and Valanginian-Aptian depocentres (Fig. 7A, B). The combined structural framework is shown in Figure 9B. The basins that formed in response to these faults must have remained sediment starved during the Late Jurassic, especially to the northwest (Fig. 9B) as most of the basin-fill occurred during the Valanginian-Aptian transgressive cycle (Figs. 7B and 9C; see also Fig. 8).

Late Jurassic faults that formed away from pre-existing Triassic faults strike NE-SW to ENE-WSW (Figs. 7A, 8, 9B and 10B). In the vicinity of Triassic faults, however, the Jurassic faults exhibit various orientations. Triassic fault 1, for example, is overlain by a right-stepping soft-linked array of NNW-SSE-striking faults (Fig. 9A, B). Middle Jurassic strata, which predate Late Jurassic activity, have been eroded partly from the footwall of Triassic fault 1 (Fig. 8). Projecting the top of the Middle Jurassic in the footwall towards the fault plane yields a throw of c. 250 ms TWTT (c. 375 m), which must have developed during Late Jurassic extension in addition to Early Triassic offset. This indicates Triassic fault 1 was reactivated during Late Jurassic extension (Fig. 10).

The northern segment of the VFZ is juxtaposed to a long, NNE-trending half-graben filled with more than a kilometre of Upper Jurassic (syn-rift) to Aptian (intra-rift) sediments (Figs. 2, 5B). The Valanginian-Aptian isopach map shows a series of depocentres along the northern segment (Fig. 7B). The largest of these is positioned adjacent to the centre of the segment. Since the Valanginian-Aptian fills in Jurassic rift topography, it can be concluded that a single, composite hanging wall depocentre had formed along the length of the northern segment in Late Jurassic times (Fig. 9B).

Upper Jurassic growth strata exist in the hanging wall to the central segment (Fig. 8), whereas reflections of the underlying Triassic-Lower Jurassic are continuous and parallel with no indication of fault activity (Figs. 5C and 8; see previous section).

This suggests that a transfer fault between the precursors to the northern and southern segment first developed at this time.

NE-SW-striking faults observed in the hanging wall of the southern segment are also present in the footwall, as a more or less continuous trend (Figs. 5A, 7A and 9B). Growth of Upper Jurassic strata in Figure 5D indicates that Late Jurassic fault activity did occur along the southern segment of the VFZ. Such Upper Jurassic wedges are, however, only small along the southern segment (Fig. 9B) and the Valanginian-Aptian isopach is thin or absent. This indicates that Late Jurassic fault activity did not produce a continuous fault there.

4.4 Lower Albian tectonostratigraphy of the North Træna Basin

The location of the principal depocentres of the Lower Albian interval is generally similar to the preceding interval (Fig. 7B and C). The thickness of the Lower Albian varies from 0 to 800 m; such thickness changes occur gradually over a distance of 15 – 20 km. The vast majority of Late Jurassic faults are truncated, or draped, by the Base Albian horizon (Fig. 6C) and the remaining rift topography is effectively filled in by the Lower Albian (Figs. 2 and 8). Only the VFZ and the ERFZ offset the Lower Albian (Figs. 2 and 8). Middle Jurassic to Lower Albian strata exhibit no difference in thickness between foot- and hanging wall of the ERFZ (Fig. 11), suggesting that the fault was largely inactive during this time.

In the northern part of the basin, the Lower Albian takes the shape of a prominent wedge that thins progressively westward, from up to a kilometre thick adjacent to the VFZ, to less than 100 m in the middle of 3-D survey I (Fig. 2). Despite this thickening of the Lower Albian towards the fault, its reflections are non-rotational, indicating onlap and stratigraphic progradation. This geometry can be explained as a result of compaction of underlying mud-rich Jurassic-Cretaceous successions, producing subsidence adjacent to the VFZ without fault activity.

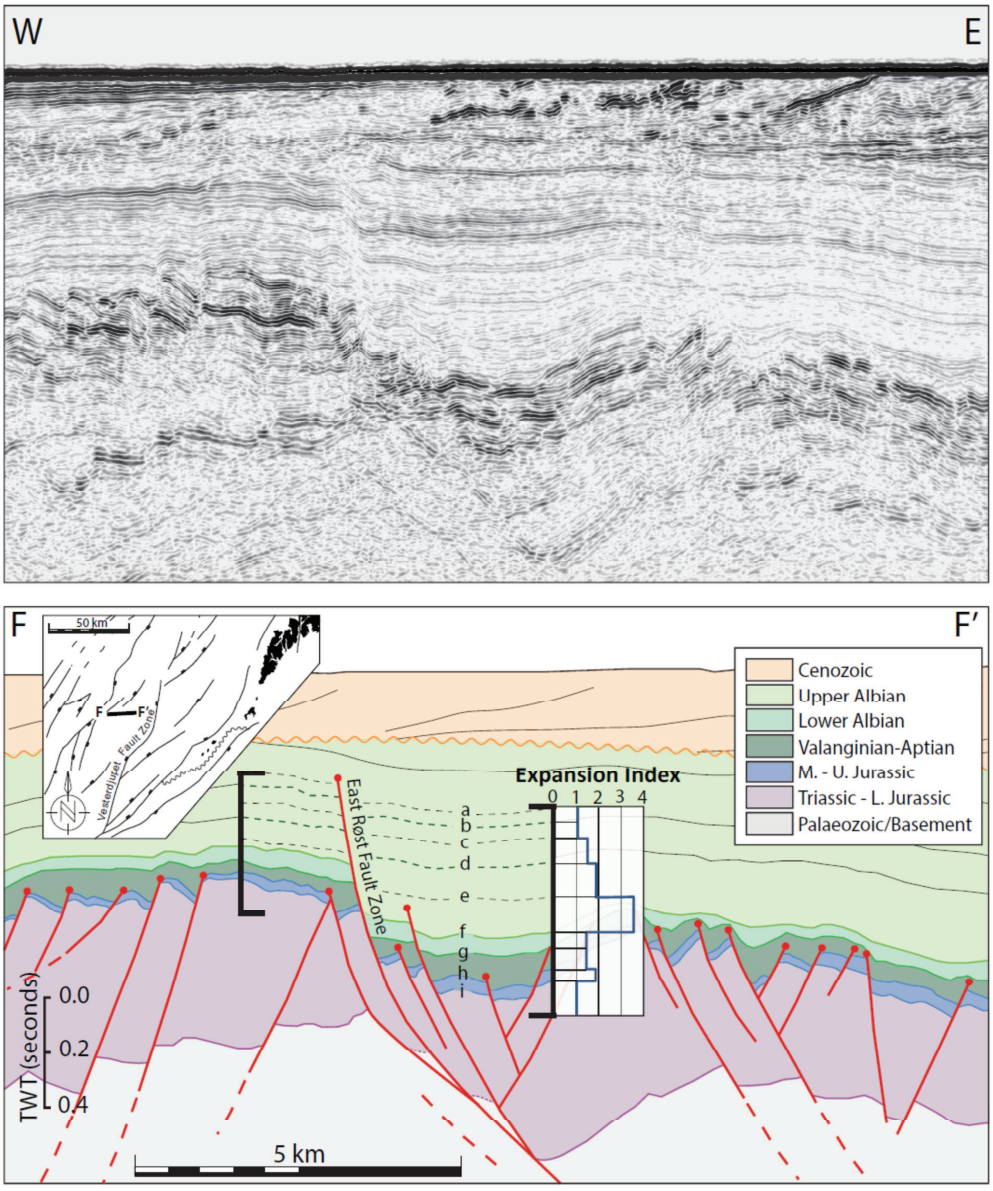

Fig. 11. *Geoseismic section F-F'. Expansion index plot across the ERFZ; see text for details. Nine horizons have been included for calculating expansion indices (a-e: intra-Upper Albian; f: mid-Albian; g: Base Albian; h: Base Cretaceous; i: Base Jurassic).*

4.5 Upper Albian tectonostratigraphy of the North Træna Basin

4.5.1 Late Albian activity of the ERFZ

The ERFZ tips out laterally to the south (Fig. 6D), and vertically it terminates within the Upper Albian succession. 3-D survey I provides a unique opportunity to study fault activity as individual reflections in its hanging wall can be mapped around the southern fault tip, onto the footwall. Six intra-Albian events (‘a’-‘f’; Fig. 11) have been mapped locally for calculating expansion indices. Expansion indices are greatest just above the mid-Albian horizon with an expansion factor >3. Thickening diminishes upward. This tells us that accommodation was generated just prior to (or during) deposition of the interval between ‘e’ and ‘f’. There is significant thickening of Upper Albian strata over the ERFZ (Fig. 7D), yet there is no stratigraphic growth in its hanging wall.

The absence of growth strata indicates that the North Træna Basin subsided uniformly over a large area as a graben rather than a half-graben, suggesting simultaneous activity of both the western (ERFZ) and eastern (VFZ) border faults. Thicker strata in the hanging wall are therefore probably the result of a higher sedimentation rate in the deeper hanging wall. Later during the Late Albian, activity of the ERFZ ceased, as evidenced by the termination of the ERFZ within the Upper Albian. An alternative interpretation of the fault movement recorded by the expansion indices is differential compaction of sediments across this Palaeozoic-Triassic fault. In the hanging wall of the ERFZ, a thick wedge of Palaeozoic sediments is present (Figs. 2 and 9A) that is most likely absent in the footwall. Compaction of these sediments could explain an increased subsidence rate east of the ERFZ, without any extension. This would fit with the lack of observations Upper Albian growth strata that would follow from extensional rotation of the ERFZ. On the other hand, if compaction of Palaeozoic sediments creates differential subsidence across the ERFZ, this should also have occurred to a certain degree when the underlying Mesozoic

sequences were being deposited. These have more or less similar thicknesses on either side of the ERFZ; differential compaction seems therefore unlikely to be the cause of renewed activity.

4.5.2 Late Albian activity of the VFZ

A continuous depocentre existed along the length of the fault zone in Late Albian times (Fig. 7D). Unfortunately, expansion indices cannot be calculated as the footwall of the VFZ does not contain Lower Cretaceous strata. The seismic expression of the upper part of this interval along the northern segment comprises a series of vertically stacked westward thinning wedges (Fig. 12). Reflections are discontinuous and exhibit downlapping in westerly direction, along with erosional surfaces. Upper Albian strata have been drilled up-dip, which were interpreted to have been deposited in an outer shelf environment. The wedges adjacent to the VFZ are therefore interpreted to reflect deposition of locally derived sediment in a high energy, deep marine environment. The development of a hanging wall depocentre filled in by locally derived sediment means that relief between foot- and hanging wall became enhanced; this suggests activity of the northern segment at this time (see also: Prosser, 1993). This is confirmed by the presence of syn-rotational strata in the uppermost Albian interval towards the southern tip of the northern segment (Fig. 8). NNE-trending structures have existed there since the Early Triassic rift episode (Fig. 9); it is likely that these were reactivated.

In the hanging wall to the southern segment of the VFZ, the Upper Albian is in stratigraphic contact with the Middle Jurassic in places. Whereas the Valanginian – Aptian and Lower Albian successions are thin or absent west of the southern segment (Fig. 7B and C), Upper Albian sediments are deposited more widely (Fig. 7D). The southern portion of the basin had thus maintained a platform setting during Late Jurassic to Middle Albian times, with little to no extensional faulting generating accommodation since Triassic times. The fact that a more continuous Upper Albian depocentre exists along the southern segment suggests that it became active at this

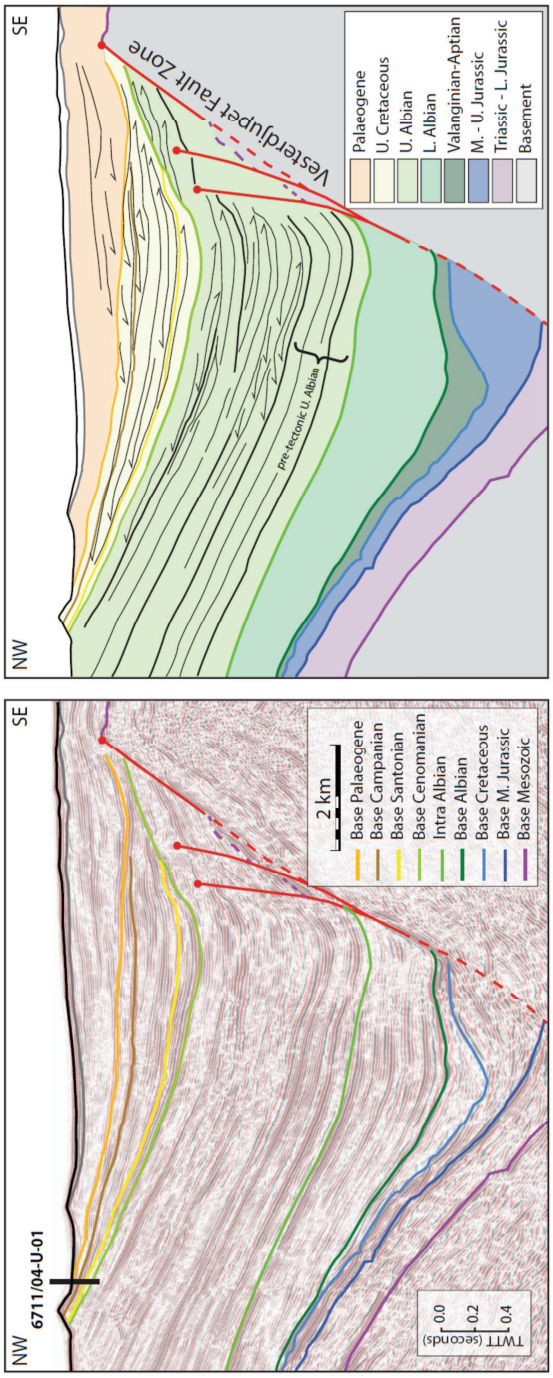

Fig. 12. *Detail of seismic line A-A' with onlap-, downlap- and erosional contacts within the Upper Albian, Upper Cretaceous and Palaeogene close to the VFZ.*

time. The southern segment is truncated at the top by the middle Cenomanian horizon and that both foot- and hanging wall are draped by Cenomanian and younger sediments (Fig. 5D). The Upper Albian depocentre must thus have formed between middle Albian and Cenomanian times. It is therefore concluded that activity of the southern segment is restricted to the Late Albian. It likely reactivated the Triassic NNE-SSW-trending structure that existed there (Triassic fault 1 and its southern extension; Fig. 5C and D).

The central segment consists of a single fault plane (Fig. 5C) juxtaposing a 1-2 km thick, Upper Albian package (Fig. 7D). The thickness of this package shows no change at the transition to the adjacent fault segments; it thus seems plausible that all segments of the VFZ had linked up, forming a through-going feature towards the end of the Albian.

4.6 Upper Cretaceous tectonostratigraphy of the North Træna Basin

The Cenomanian-Santonian intra-rift succession is characterized by onlap of the Base Cenomanian (Fig. 12). Depocenters of this interval are non-fault bounded and occur over the hanging wall depocentres (Fig. 2) hinting at compaction-driven subsidence. Minor offset of the Base Cenomanian horizon is observed for the central segment of the VFZ (Fig. 5C). This was likely accomplished by local reactivation during the Campanian-Palaeogene rift episode.

5. Discussion

5.1 Mesozoic structural inheritance in the North Træna Basin

5.1.1 The Early Triassic rift episode

A direct link between Palaeozoic extensional structures and Mesozoic rift faults has been postulated for the Lofoten margin by Olesen et al. (2002) and Eig (2012).

Triassic faults preferentially formed over the Palaeozoic substratum (Figs. 2 and 9A); we speculate that this is caused by the Palaeozoic sediments being rheologically weaker than the crystalline basement. The N-S trending ERFZ is often considered to reflect the main Triassic fault trend (e.g. Bergh et al., 2007; Hansen et al., 2012); however, although some minor movement took place in the Triassic (Triassic fault 2 in Fig. 10A), this fault is herein dated as a predominantly Late Albian feature that most likely reactivated a deep-seated Palaeozoic structure (Fig. 11).

5.1.2 The Middle-Late Jurassic rift episode

The Late Jurassic faults of the North Træna Basin exhibit a predisposition to reactivate Triassic structures. Triassic fault 1 was reactivated in Late Jurassic times (Figs. 8 and 10), as documented by the deposition of syn-rotational Upper Jurassic strata. It follows that faults formed through reactivation typically form right-stepping en echelon fault arrays striking NNW-SSE, N-S and NNE-SSW; non-reactivated faults strike NE-SW to E-W (Fig. 10).

The development of en-echelon fault arrays as a result of the oblique reactivation of pre-existing structures has been documented in scaled lab experiments (Clifton et al., 2000; Keep and McClay, 1997). Their results closely resemble the structural style of the Late Jurassic rift episode depicted in Figure 10. It is also a key feature of the coherent fault model. We therefore conclude that certain NNE-trending Triassic faults propagated upward during Late Jurassic extension, together with the inception of ENE-WSW- and E-W-striking faults.

5.1.3 The Late Albian rift episode

Except for the timing of linkage, our model for the evolution of the VFZ (Fig.13) agrees with that of Bergh et al. (2007), Eig and Bergh (2011) and Færseth (2012), who also concluded that the NE-SW-striking central segment is younger than the NNE-SSW-striking southern and northern segments. Rather than having evolved

simultaneously, the central segment formed as a transfer fault between reactivated older fault segments.

Late Albian displacement along the central segment of the VFZ, as well as the northern and southern segments, was influenced by the pre-Cretaceous structural grain but through contrasting mechanisms. The northern and southern segments, on the other hand, formed by (oblique) reactivation and linkage through breaching narrow (<2 km; Fig. 9B) relays between ancestral Triassic/Jurassic faults at depth. In contrast, the Late Jurassic transfer fault that breached the broad (c. 11 km; Fig. 5A) ramp that separates the northern and

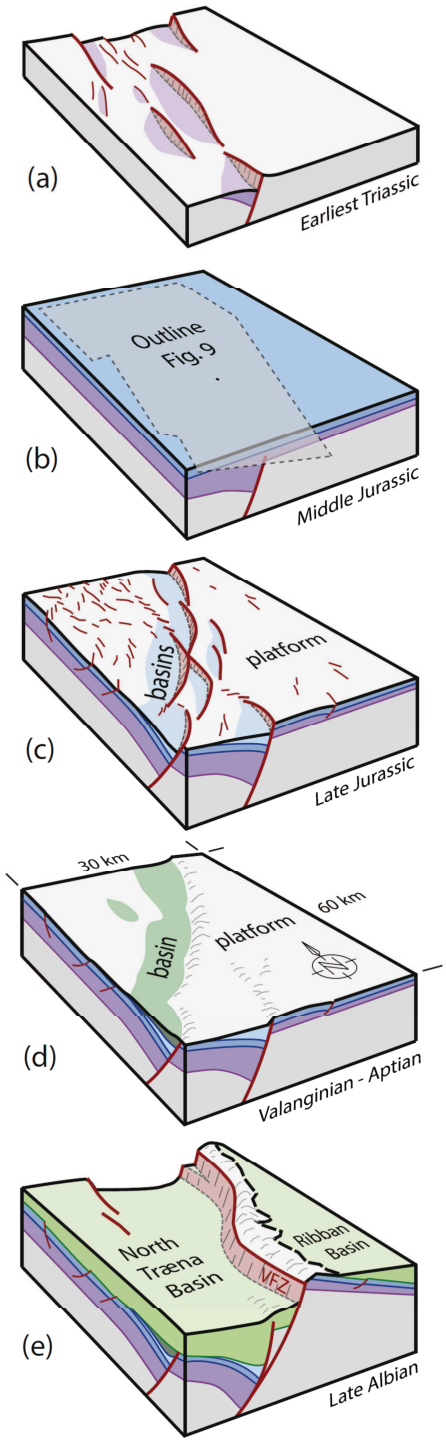

Fig. 13. *Schematic representation of the physiography of the North Basin in Early Triassic, Middle Jurassic, Late Jurassic, Late Aptian and Late Albian times. The structural framework for the Early Triassic (a), Late Jurassic (c) and Late Albian (e) are taken from Figure 9 (the outline of Figure 9 is given in (b). Note how Early Triassic faults assume a NNE-SSW orientation, while late Jurassic faults strike NE-SW predominantly. The VFZ, that emerged as a through-going fault zone towards the Late Albian, exploited both Triassic and Jurassic fault trends.*

southern segments formed (and was later reactivated) as a single structure. This may explain the lateral difference in morphology (Fig. 5), with the central segment evolving as a single fault plane whereas the northern segment and, to a lesser degree, the southern segment are composed of a series of faults and terraces. Reactivation producing more complex fault geometries than orthogonal reactivation has been observed in physical models (Keep and McClay, 1997; Henza et al., 2011), numerical models (Brune, 2014) and in natural rifts (Morley et al., 2004).

5.1.3 The Campanian-Palaeocene rift episode

We demonstrate how the locus of activity along the VFZ during the final rift episode was on the central segment, which had become the centre of the fault zone. In a similar study, Faure Walker et al. (2009) observed the removal of an original deficit of throw of a linkage zone during normal fault evolution. These workers argued that a position at the centre of an active, recently linked fault guarantees a high strain rate. The same kinematic argument was presented by Gupta and Scholz (2000), who stated that the displacement maximum is likely to be the last place to accumulate strain; this is particularly true for the VFZ. The stress regime had also changed favorably for activity along NE-trending structures (Mosar et al., 2002).

5.2 The origin of segmented faults with zigzag geometry in physical models

A series of analogue experiments in which wet clay models were subjected to two successive phases of extension with a 45° difference in extension direction were conducted by Henza et al. (2011). In these experiments, secondary structures nucleated at an angle to first-phase structures during second-phase extension, thus promoting fault linkage (Fig. 14). Depending on the relative magnitude of extension between the two phases the resultant linked fault systems were dominated by either first-phase or second-phase segments. Linkage during non-coaxial extension thus

occurs irrespective of length and separation of original first-phase structures, producing faults with strong zigzag or cross-cutting geometries.

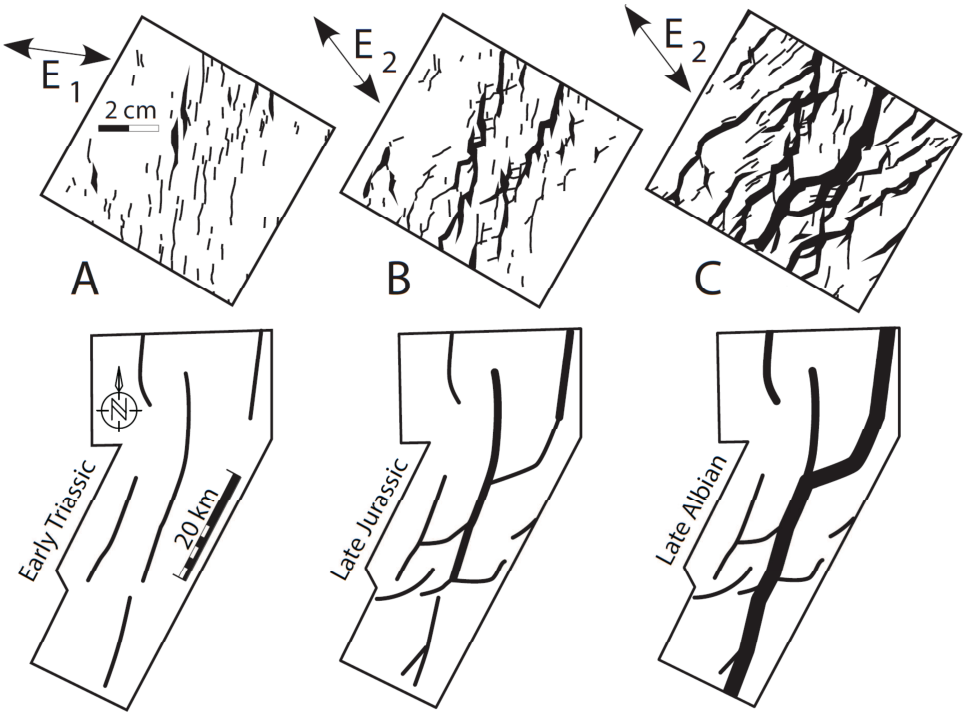

Fig. 14. *Schematic representation of the structural evolution of the North Træna Basin and the VFZ through the Mesozoic based on Figure 9 (below), compared to clay experiments of multi-stage extension by Henza et al. (2011; above). In the specific clay experiment depicted here, two phases of extension were applied; the second phase double the magnitude of the first. E_1 and E_2 indicate extension directions 1 and 2. The clay model maps have been rotated (120 degrees) to match the attitude of structures to those of the North Træna Basin, for better comparison. (A) The physical model at the end of extension phase one (above) compared to the structural framework at the end of the Early Triassic rift episode (below). (B) The physical model halfway extension phase two (above) compared to the structural framework at the end of the Late Jurassic rift episode (below). (C) The physical model at the end of extension phase two (above) compared to the structural framework at the end of the Late Albian rift episode (below).*

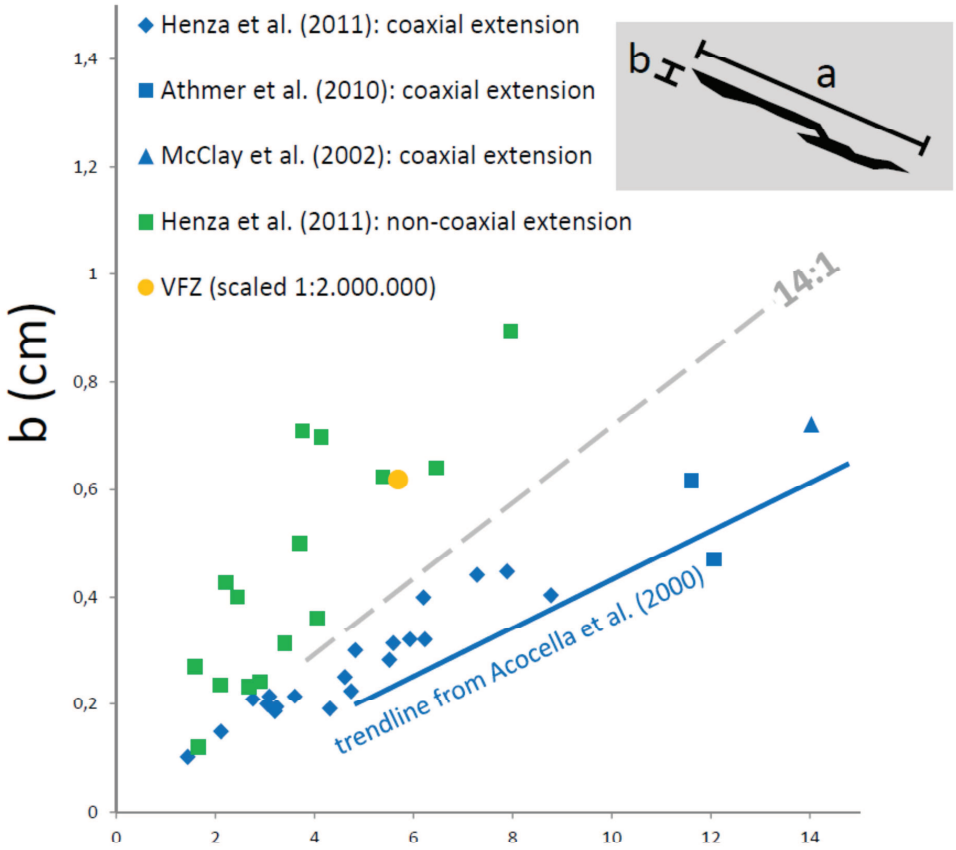

Fig. 15. *Collection of data quantifying the aspect ratio of two parallel, linked faults; their combined length ('a'; x-axis) is plotted against the width of their strike-normal separation ('b'; y-axis). The graph contains data from physical analogue models (McClay et al., 2002; Athmer et al., 2010 and Henza et al., 2011) and natural rifts (Acocella et al., 2000). Single phase refers to co-axial extension, multiphase refers to non-coaxial extension. The stippled line indicates the 14:1 aspect ratio between combined fault length and separation.*

In experiments that lacked a change in extension direction, faults typically grew laterally at the tips. Linkage occurred incidentally when growing, parallel faults began to overlap and interact. With no pre-existing structure to be reactivated, these faults are best described as having formed following the isolated fault model. One important characteristic of experiments simulating coaxial (uniform) extension is that overlapping faults only link up when their strike-normal spacing is relatively modest;

linked systems retained an overall parallel appearance (Henza et al., 2011; see also Keep and McClay 1997; McClay et al., 2002).

Figure 15 provides empirical data from physical models to illustrate the relationship between the combined length of two linked, first-phase faults and their strike-normal separation (respectively ‘a’ and ‘b’; Fig. 15). The graph reveals a strong split between results from coaxial and non-coaxial extension models. A boundary between both groups can be drawn along the 14:1 line (Fig. 15). It can thus be concluded that overlapping, parallel faults, which started off as isolated features, did not link up during coaxial extension if their separation exceeded c. 8% of their combined length. A critical length for linkage of parallel fault segments was also obtained from analysis of segmented normal faults in Upper Pleistocene to Holocene basalts on Iceland (Acocella et al., 2000). Given their young age, these faults likely developed under uniform (coaxial) extension. The linear best-fit line of the Icelandic data overlaps with the results of experiments simulating coaxial extension (Fig. 15). Data from the natural faults in Iceland display a larger spread than the physical models; nevertheless, these workers also suggested a minimal combined segment length of 14 times their separation in order for interaction to occur.

5.3 Models explaining the plan-view geometry of the Vesterdjupet Fault Zone

5.3.1 Fault linkage following the isolated fault model

Fault systems evolving following the isolated fault model, without a change in the extension vector or inherent weaknesses in the substratum, tend to be rather linear as shown in the previous section. For the VFZ, the length of the connected southern and northern segment is 114 km (Figs. 1 and 5A) and their separation c. 11 km (Fig. 5A). This yields a ratio of roughly 10:1; when scaled, the VFZ plots within the domain of non-coaxial extension (Fig. 15).

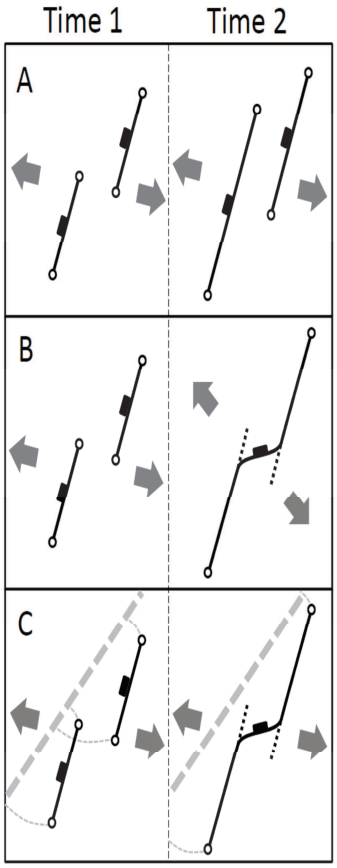

Fig. 16. *Different models that can explain the emergence of zigzag plan-view geometry of normal faults which evolve during multiphase rifting. (A) Two faults developing according to the isolated fault model; their length and separation is such that they do not interact as extension progresses. (B) Two faults developing according to the isolated fault model; as the direction of extension changes favourably for a transfer fault to develop, the faults link up. (C) A pre-existing structure at depth is reactivated obliquely; although the faults at surface appear soft-linked, they are in fact hard-linked at depth and will likely link when extension increases.*

Local deflection of least principal stress may be caused by interaction of overlapping faults (Morley et al., 1990; Brune, 2014). In the North Træna Basin, at least one example of such a local perturbation of the least principal stress vector is observed. In the overlap area between Triassic faults 1 and 2 (Figs. 9A, B and 10A, B), the plan-view network of relatively small Late Jurassic faults resembles that of a convergent, overlapping transfer zone as described by Morley et al. (1990). If we assume that for natural rifts the same critical relationship of 14:1 exists between fault length and segment separation, as the work of Acocella et al. (2000) suggests, then the spacing of the Triassic precursors of the northern and southern segments of the VFZ would be too wide (10:1) for the stress field to be perturbed in such a way that it promotes interaction between these faults (Fig. 16A). Speculating further under this assumption, the fact that segment linkage did occur in Late Jurassic to Early

Cretaceous times implies i) a more widespread, favourable change in the orientation of least principal stress (Fig. 16B) and/or ii) the presence of inherent weaknesses in the basement (Fig. 16C).

5.3.2 Stress rotation

The VFZ has a plan-view expression that is very similar to the end result of clay model C from Henza et al. (2011), which is therefore chosen as analogue. Three different stages of model C are compared to the multiphase evolution of the North Træna Basin (Fig. 14). Despite the limitations of scaled analogue experiments, the clay model model, and its controlled environment, reveals that the zigzag geometry of the VFZ could be explained as a consequence of a change in extension direction between rift episodes.

A rotation of the sub-regional stress field has been invoked between the Early Triassic and Late Jurassic rift episodes (e.g. Faleide et al., 2008). The favourable, c. 30°-50° clockwise rotation of the least principal stress suggested by these workers could explain the linkage of relatively wide-spaced Triassic faults in the manner observed in physical models of non-coaxial extension. Sub-regional rotations of the stress field are often invoked in order to explain non-collinear fault populations in the Norwegian passive margin (e.g. Færseth et al., 1997; Doré et al., 1997; Davies et al., 2001). Reeve et al. (2015) argue that such major rotations in extension direction are not always required to explain different fault populations developing simultaneously as intra-basement weaknesses can often account for local perturbations of the stress field. Although the observation of a difference in orientation between Jurassic and Triassic faults is also made in the present study (Fig. 9A, B), there exists no independent evidence for stress rotation in the Lofoten margin between the Triassic and Jurassic rift episodes (Mosar et al., 2002; Færseth, 2012). For the VFZ this means that, although the invoked regional stress rotation offers an elegant explanation for the zigzag geometry of the VFZ, it cannot be proven independently at this point and

the possibility of more local stress perturbations facilitating fault linkage should not be discarded.

5.3.3 Influence of basement weaknesses

We have not found evidence which either proves or disproves that the Triassic precursors to the VFZ were influenced by basement weaknesses as Wilson et al. (2006) suggest. If the Triassic faults did in fact develop along a NE-trending basement weakness, their linkage in Late Jurassic to Early Cretaceous times can be explained as reactivation of an already kinematically linked fault system (Fig. 16C). Such a setting in which extension over a buried weakness zone influences the geometry of subsequent normal faults was recreated in the physical analogue models of Hus et al. (2005). Faults developed over a weakness zone that linked up even if their combined length was only eight times their separation.

NE-trending Caledonian basement lineaments, known onshore, are suggested to have influence Mesozoic rifting (e.g. Doré et al., 1997; Wilson et al., 2006). There are, however, indications that no such pre-existing structural grain exists underneath the North Træna Basin. The VFZ at the eastern edge of the basin is underlain by a crystalline basement dome that forms part of a metamorphic core complex (Henstra and Rotevatn, 2014). This exhumed lower crust typically lacks any tectonic imprint of Caledonian age in the Lofoten area (Hames & Andresen 1996; Steltenpohl et al., 2006). It is therefore possible that the Triassic precursors to the VFZ nucleated as isolated features in a substrate without zones of weakness. In that case, their linkage in Late Jurassic to Early Cretaceous times can be explained by comparison to models of non-coaxial extension that also lack a pre-rift structural grain.

6. Summary and conclusions

A detailed model for the polyphase evolution of a major rift border fault is provided based on interpretation of 2-D and 3-D seismic data over the North Træna Basin.

- During the Early Triassic rift episode, E-W-directed extension resulted in the development of NNE-SSW-striking faults. In the subsequent Late Jurassic and Early Cretaceous rift episodes, ENE-WSW- to E-W-striking faults formed while certain Triassic faults were reactivated. The presence and geometry of Triassic structures influenced the style of Late Jurassic fault growth, which in turn controlled the architecture of the Cretaceous VFZ.
- A comparison to physical analogue models of non-coaxial extension reveals several similarities: i) the orientation of early structures dominate the geometry of late stage linked faults and ii) the late stage establishment of a single fault zone with zigzag geometry from the previously linked fault framework.
- Given the relatively wide strike-perpendicular spacing of the original segments and the likely homogenous nature of crystalline basement, we suggest that a previously invoked stress rotation in Jurassic times introduced non-coaxial extension between the Triassic and later rift episodes. This lead to the observed zigzag-style linkage.

Our analysis of the VFZ contributes to the wider understanding of normal fault growth in multi-rift systems and highlights the role of pre-existing fault segments and their reactivation in controlling the overall geometry of large, basin-bounding fault zones formed over multiple phases of extension.

Acknowledgements

We acknowledge Shell Norway for providing data access and funding for this study. Schlumberger is thanked for licensing the Petrel software package to the University of Bergen allowing in-house seismic interpretation. Permission to publish 2-D data was granted by TGS; the 3-D data by PL219 partners. We salute Peter Bormann, Marius Brundiers and Ben Hull-Bailey for instructive discussions and help at the start-up phase of seismic interpretation. Christian Haug Eide and Jord de Boer at the University of Bergen are thanked for suggested figure improvements. The article benefited from thorough reviews by Chris Jackson, Chris Morley and Toru Takeshita.

References

Acocella, V., Gudmundsson, A., Funiciello, R., 2000. Interaction and linkage of extension fractures and normal faults: examples from the rift zone of Iceland. Journal of Structural Geology 22, 1233-1246.

Andersen, T.B., Jamtveit, B., Dewey, J.F., Swenson, E., 1991, Subduction and eduction of continental crust: Major mechanisms during continent-continent collision and orogenic extensional collapse, a model based on the southern Norwegian Caledonides. Terra Nova 3, 303-310.

Athmer, W., Groenenberg, R.M., Luthi, S.M., Donselaar, M.E., Sokoutis, D., Willingshofer, E., 2010. Relay ramps as pathways for turbidity currents: a study combining analogue sandbox experiments and numerical flow simulations. Sedimentology 57, 806–823.

Bergh, S.G., Eig, K., Kløvjan, O.S., Henningsen, T., Olesen, O., Hansen, J.-A., 2007. The Lofoten-Vesterålen continental margin: a multiphase Mesozoic-Palaeogene rifted shelf as shown by offshore-onshore brittle fault-fracture analysis. Norwegian Journal of Geology 87, 29-58.

Blystad, P., Brekke, H., Færseth, R.B., Larsen, B.T., Skogseid, J., Tørudbakken, B., 1995. Structural elements of the Norwegian continental shelf. Part II: The Norwegian Sea Region. Norwegian Petroleum Directorate Bulletin 8, 1-45.

Brekke, H., 2000. The tectonic evolution of the Norwegian Sea Continental Margin with emphasis on the Vøring and Møre Basins. In: Nøttvedt, A. (Ed.), Dynamics of the Norwegian Margin. Geological Society, London, Special Publication 167, 327-378.

Brune, S., 2014.Evolution of stress and fault patterns in oblique rift systems: 3D numerical lithospheric-scale experiments from rift to breakup. Geochemistry Geophysics Geosystems 15, 3392–3415.

Cartwright, J.A., Mansfeld, C., Trudgill, B., 1996. The growth of normal faults by segment linkage. In: Buchanan, P.G., Nieuwland, D.A. (Eds.), Modern developments in structural interpretation, validation and modeling. Geological Society, London, Special Publication 99, 163-177

Childs, C., Watterson, J., Walsh, J.J., 1995. Fault overlap zones within developing normal fault systems. Journal of the Geological Society of London 152, 535–549.

Clifton, A.E., Schlische, R.W., Withjack, M.O., Ackermann, R.V., 2000. Influence of rift obliquity on fault-population systematics: results of experimental clay models. Journal of Structural Geology 22, 1491-1509.

Coward, M.P., Dewwey, J.R., Hempton, M., Holroyd, J., Mange, M.A., 2003. Chapter 2: Tectonic Evolution. In: Evans, D., Graham, C., Armour, A., Bathurst P. (Eds.), The Millenium Atlas: petroleum geology of the central and northern North Sea. The Geological Society of London, London, 17-33.

Cowie, P.A., Gupta, S., Dawers, N. H., 2000. Implications of fault array evolution for synrift depocentre development: insights from a numerical fault growth model. Basin Research 12, 241–261.

Crider, J.G., Pollard, D.D., 1998. Fault linkage: Three-dimensional mechanical interaction between echelon normal faults. Journal of Geophysical Research 103, 24,373-24,391.

Davies, R.J., Turner, J.D., Underhill, J.R., 2001. Sequential dip-slip fault movement during rifting: a new model for the evolution of the Jurassic trilete North Sea rift system. Pet. Geosci. 7, 371-388.

Doré, A.G., 1992. Synoptic palaeogeography of the Northeast Atlantic Seaway: late Permian to Cretaceous. In: Parnell, J. (Ed.), Basins on the Atlantic Seaboard: Petroleum Geology, Sedimentology and Basin Evolution. Geological Society, London, Special Publications 62, 421-446.

Doré, A.G., Lundin, E.R., Fichler, C., Olesen, O., 1997. Patterns of basement structure and reactivation along the NE Atlantic margin. Journal of the Geological Society 154, 85-92.

Doré, A.G., Lundin, E.R., Jensen, L.N., Birkeland, Ø., Eliassen, P.E., Fichler, C., 1999. Principal tectonic events in the evolution of the northwest European Atlantic margin. In: Fleet, A.J., Boldy, S.A. (Eds.), Petroleum Geology of Northwest Europe. Proceedings of the 5th Conference, 41-62.

Dubois, A., Odonne, F., Massonnat, G., Lebourg, T., Fabre, R., 2002. Analogue modelling of fault reactivation: tectonic inversion and oblique remobilization of grabens. Journal of Structural Geology 24, 1741-1752.

Eidvin, T., Brekke, H., Riis, F., Renshaw, D.K., 1998. Cenozoic stratigraphy of the Norwegian Sea continental shelf, 64°N-68°N. Norwegian Journal of Geology 78, 125-151.

Eig, K., 2012. Lofoten and Vesterålen: Promised Land or Fata Morgana? GEo ExPro 9, 54-59.

Eig, K., Bergh, S.G., 2011. Late Cretaceous–Cenozoic fracturing in Lofoten, North Norway: Tectonic significance, fracture mechanisms and controlling factors. Tectonophysics 499, 190-205.

Faleide, J.I., Tsikalas, F., Breivik, A.J., Mjelde, R., Ritzmann, O., Engen, Ø., Wilson, J., Eldholm, O., 2008. Structure and evolution of the continental margin off Norway and the Barents Sea. Episodes 31, 82-90.

Faleide, J.I., Bjørlykke, K, Gabrielsen, R.H., 2010. Geology of the Norwegian Continental Shelf. In: Bjørlykke, K.: Petroleum Geoscience: From Sedimentary Environments to Rock Physics. Springer-Verlag, Berlin Heidelberg, 467-499.

Faure Walker, J.P., Roberts, G.P., Cowie, P.A., Papanikolaou, I.D., Sammonds, P.R., Michetti, A.M., Phillips, R.J., 2009. Horizontal strain-rates and throw-rates for breached relay-zones: an example from active normal faults in the Apennines, Italy. Journal of Structural Geology 31, 1145-1160.

Fossen, H., 2000. Extensional tectonics in the Caledonides: synorogenic or postorogenic? Tectonics 19, 213–224.

Freund, R., and Merzer, A.M., 1976. The formation of rift valleys and their zigzag fault patterns. Geology Magazine 113, 561-568.

Færseth, R.B., Knudsen, B.-E., Liljedahl, T., Midbøe, P.S. and Søderstrøm, B., 1997. Oblique rifting and sequential faulting in the Jurassic development of the northern North Sea. Journal of Structural Geology 19, 1285-1302.

Færseth, R.B., Lien, T., 2002. Cretaceous evolution in the Norwegian Sea - a period of tectonic quiescence. Marine and Petroleum Geology 19, 1005–1027.

Færseth, R.B., 2012. Structural development of the continental shelf offshore Lofoten–Vesterålen, northern Norway. Norwegian Journal of Geology 92, 19-40.

Gernigon, L., Ringenbach, J.C., Planke, S., Le Gall, B., Jonquet-Kolstø, H., 2003. Extension, crustal structure and magmatism at the outer Vøring Basin, Norwegian margin. Journal of the Geological Society London 160, 197-208.

Giba, M., Walsh, J.J., Nicol, A., 2012. Segmentation and growth of an obliquely reactivated normal fault. Journal of Structural Geology 39, 253-267.

Groshong, R.H., 1999. 3-D Structural Geology - A Practical Guide to Quantitative Surface and Subsurface Map Interpretation. Springer-Verlag, Berlin.

Hames, W.E., Andresen, A., 1996. Timing of Palaeozoic orogeny and extension in the continental shelf of north-central Norway as indicated by laser 40Ar/ 39Ar muscovite dating. Geology 24, 1005-1008.

Hansen, J.W, Bakke, S., Fanavoll, S., 1992. Shallow drilling Nordland VI and VII 1992. IKU report 23.

Hansen, J.-A., Bergh, S.G., Henningsen, T. 2012. Mesozoic rifting and basin evolution on the Lofoten and Vesterålen Margin, North-Norway; time constraints and regional implications. Norwegian Journal of Geology 91, 203-228.

Henstra, G.A., Rotevatn, A., 2014. Nature of Palaeozoic extension in Lofoten, north Norwegian Continental Shelf: insights from 3-D seismic analysis of a Cordilleran-style metamorphic core complex. Terra Nova 26, 247-252.

Henza, A.A., Withjack, M.O., Schlische, R.W., 2011. How do the properties of a pre-existing normal-fault population influence fault development during a subsequent phase of extension? Journal of Structural Geology 33, 1312-1324.

Jackson, C.A-L., Gawthorpe, R.L., Sharp, I.R., 2002. Growth and linkage of the East Tanka fault zone; structural style and syn-rift stratigraphic response. Journal of the Geological Society of London 159, 175–187.

Jackson, C.A-L., Rotevatn, A., 2013. 3D seismic analysis of the structure and evolution of a salt-influenced normal fault zone: a test of competing fault growth models. Journal of Structural Geology 54, 215-234.

Keep, M., McClay, K.R., 1997, Analogue modeling of multiphase rift systems. Tectonophysics 273, 239-270.

Koch, J.-O., Heum, O.R., 1995. Exploration trends of the Halten Terrace. In: Hanslien, S. (Ed.), Petroleum Exploration and Exploitation in Norway. NPF Special Publication 4, 235-251.

Lepvrier, C., Fournier, M., Bérard, T., Roger, J., 2002. Cenozoic extension in coastal Dhofar (southern Oman): implications on the oblique rifting on the Gulf of Aden. Tectonophysics 357, 279-293.

Lundin, E.R., Doré, A.G., 1997. A tectonic model for the Norwegian passive margin with implications for the NE Atlantic: Early Cretaceous to break-up. Journal of the Geological Society London 154, 545–550.

Løseth, H., Tveten, E., 1996. Post-Caledonian structural evolution of the Lofoten and Vesterålen offshore and onshore areas. Norwegian Journal of Geology 76, 215-230.

McClay, K.R., Dooley, T., Whithouse, P., Mills, M., 2002. 4-D evolution of rift systems: insight from scaled physical models. Bulletin of the American Association of Petroleum Geologists 86, 935–959.

McLeod, A., Dawers, N.H., Underhill, J.R., 2000. The propagation and linkage of normal faults: insights from the Strathspey–Brent–Statfjord fault array, northern North Sea. Basin Research, 12, 263–284.

Morley, C.K., Nelson, R.A., Patton, T.L., Munn, S.G., 1990. Transfer zones in the East African Rift system and their relevance to hydrocarbon exploration in rifts. AAPG Bulletin 74, 1234-1253.

Morley, C. K., 1999. Patterns of displacement along large normal faults: implications for basin evolution and fault propagation, based on examples from East Africa. AAPG Bulletin 83, 613–634.

Morley, C.K., Haranya, C., Phoosongsee, W., Pongwapee, S., Kornsawan, A., Wonganan. N., 2004. Activation of rift oblique and rift parallel pre-existing fabrics during extension and their effects on deformation style: examples from the rifts of Thailand. Journal of Structural Geology 26, 1803-1829.

Morley, C.K., Gabdi, S., Seusutthiya, K., 2007. Fault superimposition and linkage resulting from stress changes during rifting: Examples from 3D seismic data, Phitsanulok Basin, Thailand. Journal of Structural Geology 29, 646-663.

Mosar, J., Eide, E.A., Osmundsen, P.T., Sommaruga, A., Torsvik, T.H., 2002. Greenland – Norway separation: A geodynamic model for the North Atlantic. Norwegian Journal of Geology 82, 281-298.

Olesen, O., Lundin, E., Nordgulen, Ø., Osmundsen, P.T., Skilbrei, J.R., Smethurst, M.A., Solli, A., Bugge, T., Fichler, C., 2002. Bridging the gap between the onshore and offshore geology in Nordland, northern Norway. Norwegian Journal of Geology 82, 243-262.

Peacock, D.C.P., Sanderson, D.J., 1991. Displacements, segment linkage and relay ramps in normal fault zones. Journal of Structural Geology 13, 721–733.

Prosser, S., 1993. Rift-related linked depositional systems and their seismic expression. In: Williams, G.D., Dobb, A. (Eds.), Tectonics and seismic sequence stratigraphy. The Geological Society of London, London, 35–66.

Ravnås, R., Nøttvedt, A., Steel, R.J., Windelstad, J., 2000. Syn-rift sedimentary architectures in the Northern North Sea. In: Nøttvedt, A. (Ed.), Dynamics of the Norwegian Margin. Geological Society, London, Special Publications 167, 133-177.

Reeve, M.T., Bell, R.E., Duffy, O., Jackson, C.A-L., Sansom, E., 2015. The development of non-colinear fault systems; what can we learn from 3D seismic reflection data? Journal of Structural Geology 70, 141-155.

Scholz, C.H., Dawers, N.H., Yu, J.-Z., Anders, M.H., 1993. Fault growth and fault scaling laws: preliminary results. Journal of Geophysical Research 98, 21,951-21,961.

Skogseid, J., Planke, S., Faleide, J.I., Pedersen, T., Eldholm, O., Neverdal, F., 2000: NE Atlantic continental rifting and volcanic margin formation. In: Nøttvedt, A. (Ed.), Dynamics of the Norwegian Margin. Geological Society, London, Special Publications 167, 295-326.

Steltenpohl, M.G., Hames, W.E., Andresen, A., 2004. The Silurian to Permian history of a metamorphic core complex in Lofoten, northern Scandinavian Caledonides. Tectonics 23, 1-23.

Steltenpohl, M.G., Kassos, G., and Andresen, A., 2006. Retrograded eclogite-facies pseudotachylites as deep-crustal paleoseismic faults within continental basement of Lofoten, north Norway. Geosphere 2, 61–72.

Surlyk, F., 2003. The Jurassic of East Greenland: a sedimentary record of thermal subsidence, onset and culmination of rifting. In: Ineson, J.R., Surlyk, F. (Eds.), The Jurassic of Denmark and Greenland. Geological Survey of Denmark and Greenland Bulletin 1, 659–722.

Thorsen, C.E., 1963. Age of growth faulting in Southeast Louisiana. Transactions Gulf Coast Association of Geological Societies 13, 103–110.

Torsvik, T.H., Mosar, J., Eide, E.A., 2001. Cretaceous-Tertiary Geodynamics: A North Atlantic Exercise. Geophysical Journal International 146, 850-866.

Torsvik, T.H., Cocks, L.R.M., 2003. Earth Geography from 400 to 250 Ma: a palaeomagnetic, faunal and facies review. Journal of the Geological Society London 161, 555-572.

Tsikalas, F., Faleide, J.I., Eldholm, O., 2001. Lateral variations in tectono-magmatic style along the Lofoten-Vesterålen volcanic margin off Norway. Marine and Petroleum Geology 18, 807-832.

Walsh, J.J., Nicol, A., Childs, C., 2002. An alternative model for growth of faults. Journal of Structural Geology 24, 1669-1675.

Walsh, J.J., Bailey, W.R., Childs, C., Nicol, A., Bonson, C.G., 2003. Formation of segmented normal faults: a 3D perspective. Journal of Structural Geology 25, 1251-1262

Whipp, P.S., Jackson, C.A-L., Gawthorpe, R.L., Dreyer, T., Quinn, D., 2014. Normal fault array evolution above a reactivated rift fabric; a subsurface example from the northern Horda Platform, Norwegian North Sea. Basin Research 26.

Wilson, R.W., McCaffrey, K.J.W., Holdsworth, R.E., Imber, J., Jones, R.R., Welbon, A.I.F., Roberts, D., 2006. Complex fault patterns, transtension and structural segmentation of the Lofoten Ridge, Norwegian margin; using digital mapping to link onshore and offshore geology. Tectonics 25, 1-28.

Young, M.J., Gawthorpe, R.L., Hardy, S., 2001. Growth and linkage of a segmented normal fault zone; the Late Jurassic Murchison-Statfjord North Fault, northern North Sea. Journal of Structural Geology 23, 1933-1952.